CKM 2023

12th INTERNATIONAL WORKSHOP ON THE CKM UNITARITY TRIANGLE

SANTIAGO DE COMPOSTELA

18-22 SEPTEMBER 2023

Top-quark spin properties at LHC

Nello Bruscino (INFN Roma)

on behalf of the ATLAS and CMS Collaborations

Top quark physics

Production time		Decay time		Hadronisation time		Spin-Decorr. time
$\frac{1}{m_t}$	$<$	$\frac{1}{\Gamma_t}$	$<$	$\frac{1}{\Lambda_{QCD}}$	$<$	$\frac{m_t}{\Lambda^2_{QCD}}$
~10^{-27} s		~10^{-25} s		~10^{-24} s		~10^{-21} s

Why top quarks?

- heaviest known particle, only "bare" quark
- high statistics allows precision tests and search for new physics (Effective Field Theory frameworks)

Copious production at the LHC (top-factory):

- ≈140/fb @13TeV collected in Run 2 by ATLAS…

$$\frac{dN}{dt} = \mathscr{L} \cdot \sigma_{t\bar{t}},$$
$$\sigma_{t\bar{t}} \approx 830\,\text{pb}, \implies$$
$$\mathscr{L} \approx 15 \cdot 10^{33}\,\text{cm}^2\,\text{s}^{-1}$$

Science 376, 170 (2022)

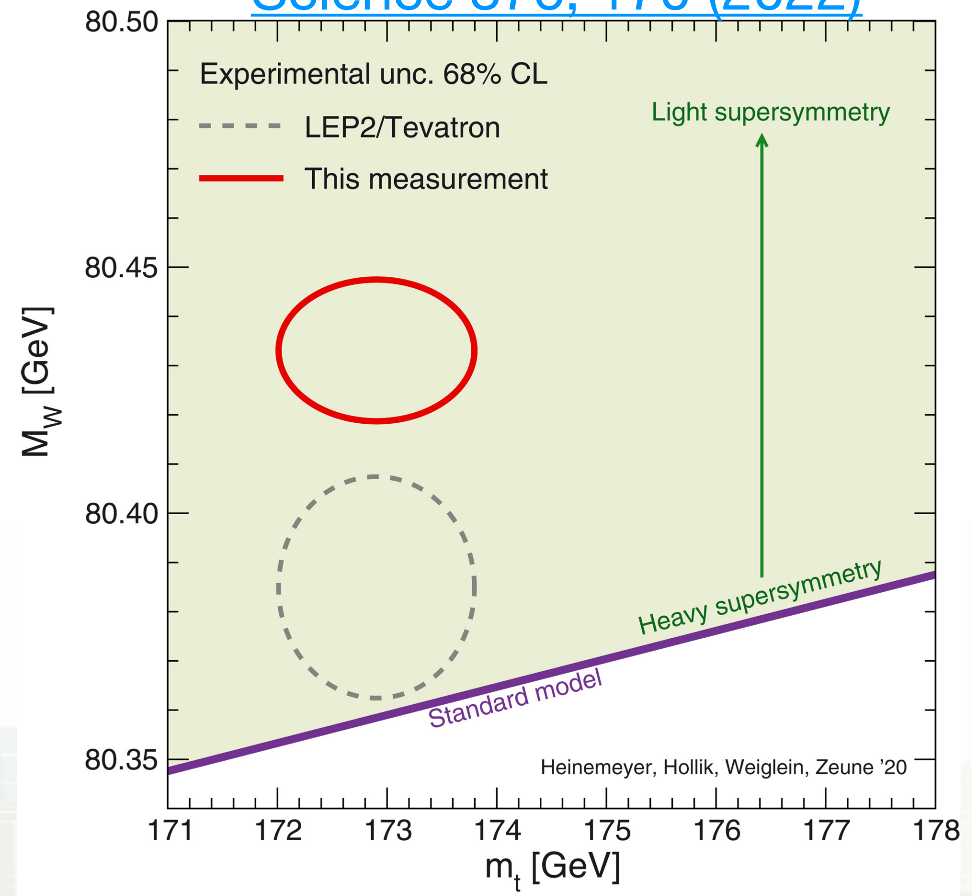

$t\bar{t}$ charge asymmetry

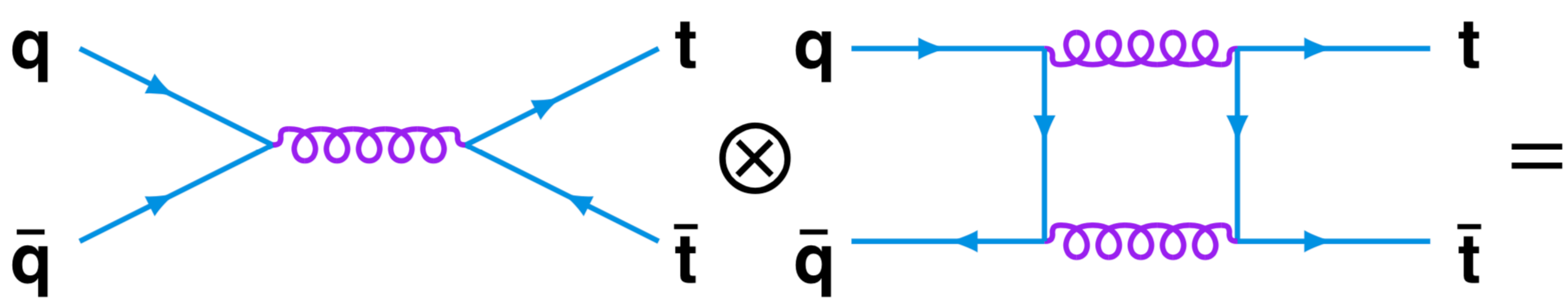

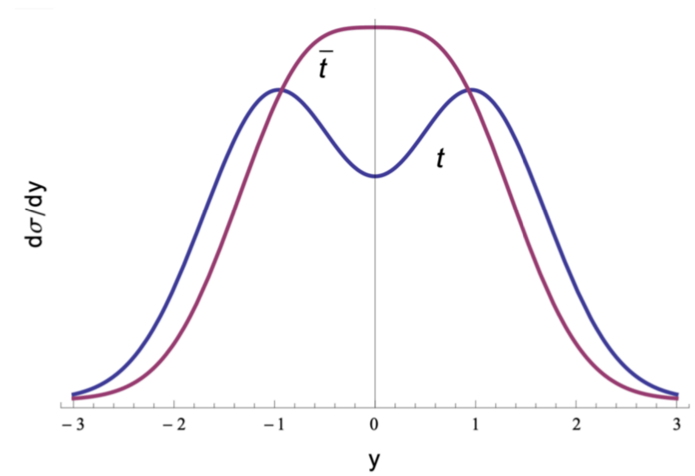

$t\bar{t}$ central–forward charge asymmetry ($A_C^{t\bar{t}}$) happens only at NLO

- gg initiated process remains charge symmetric to all orders
- higher orders interference in qg and qq̄, and EW contributions lead to asymmetries
  - also BSM physics can lead to enhancements
- challenging to measure at the LHC (qq̄ ~ 10% of production fraction @13 TeV)
  - **Extremely subtle precent-level (0.6%) effect** (one of the most precise SM tests in top physics)

$$A_C^{t\bar{t}} = \frac{N(\Delta|y|>0) - N(\Delta|y|<0)}{N(\Delta|y|>0) + N(\Delta|y|<0)} \qquad \Delta|y| = |y(t)| - |y(\bar{t})|$$

$t\bar{t}$ charge asymmetry

arXiv:2208.12095 - Accepted by JHEP

Extracted from 139/fb @13TeV data using single lepton (e/μ) and dilepton channels

- l+jets: resolved+boosted (p_T(t) ≳ 400 GeV)

Resolved: BDT to assign the different jets to the top systems

- using KLFitter, masses of hadronic top and W, various angular variables
- best combination considered and only events with good reconstruction retained

Boosted: hadronic top reconstructed as a single large-R jet

- mass and τ_{32} used to "tag" hadronic tops
- leptonic side reconstructed from the E_T^{miss}, lepton and a R=0.4 jet

Dilepton: small-R jets and exactly 2 light leptons

- Neutrino Weighting (NW) algorithm to select well reconstructed events

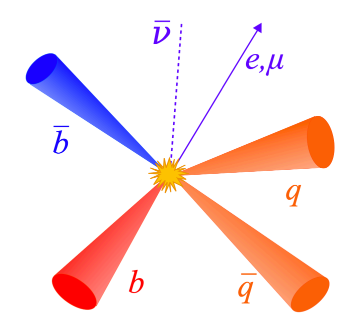

Resolved

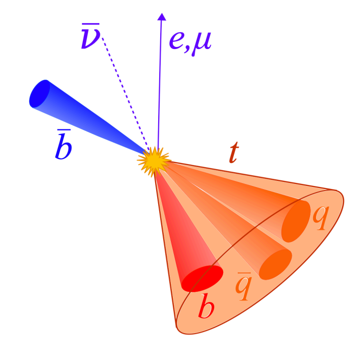

Boosted

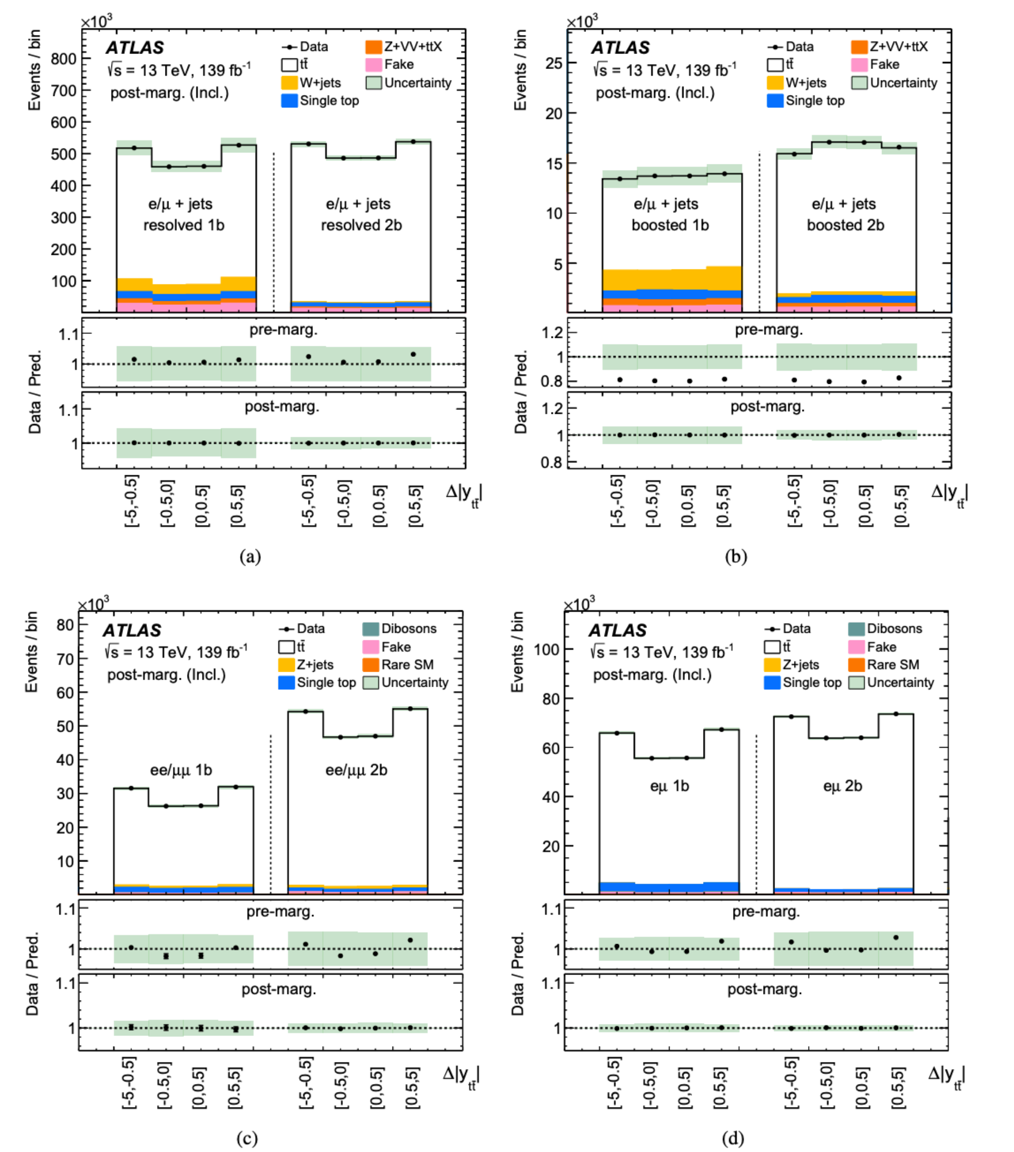

(a) (b) (c) (d)

$t\bar{t}$ charge asymmetry

arXiv:2208.12095 - Accepted by JHEP

$|\Delta y|$ unfolded using a likelihood-based technique called "fully bayesian unfolding"

- inclusive and differential in bins of the $m_{t\bar{t}}$ and $\beta_{z,t\bar{t}}$ (absolute longitudinal boost of $t\bar{t}$ system in the *z*-direction)
- systematic uncertainties are marginalised and can be constrained by the data

Inclusive charge asymmetry A_C = (0.68±0.15)%

- in agreement with NNLO QCD + NLO EW predictions
- **4.7σ from no-asymmetry hypothesis**
- EFT limits based on the inclusive and $m_{t\bar{t}}$ results

First evidence for charge asymmetry in pp collisions!

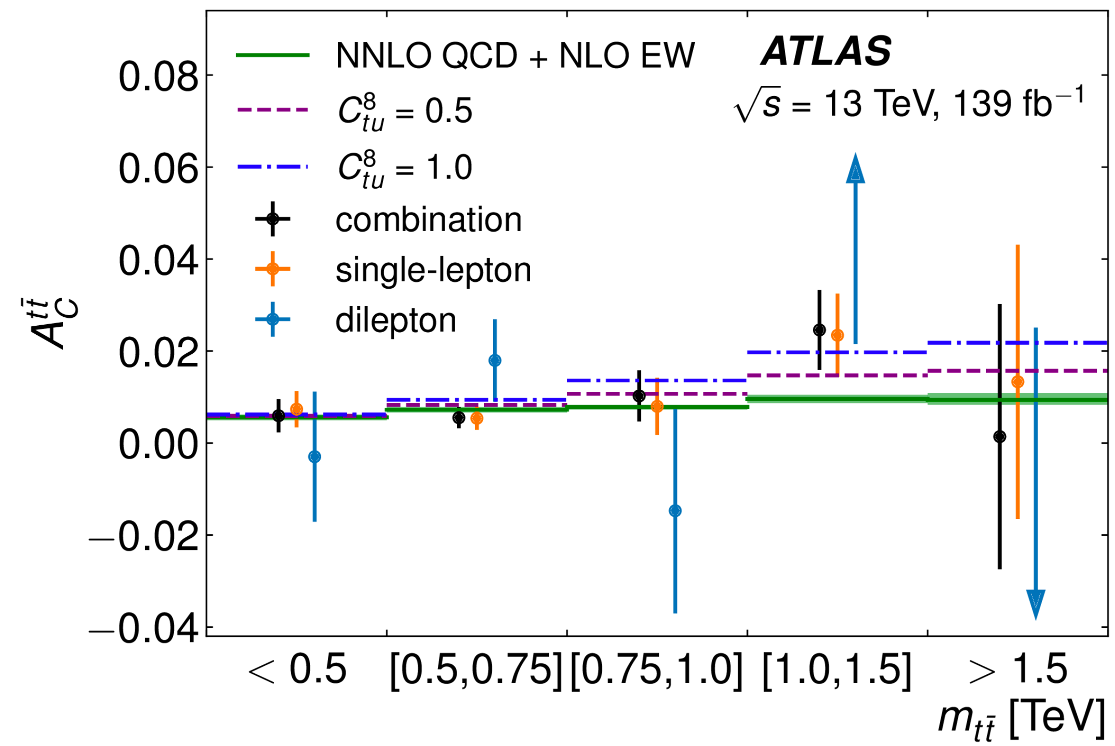

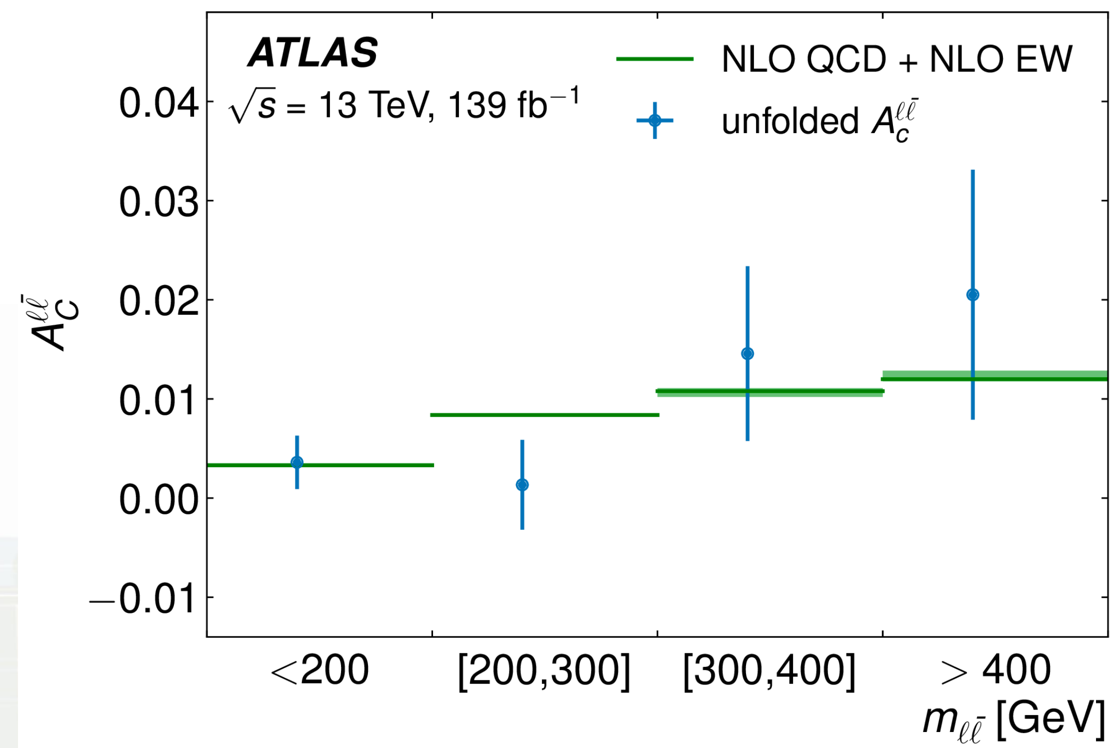

$t\bar{t}$ charge asymmetry

arXiv:2208.12095 - A

$|\Delta y|$ unfolded using a likeli
called "fully bayesian unfo

- inclusive and differential
  $\beta_{z,t\bar{t}}$ (absolute longitudina
  the *z*-direction)
- systematic uncertainties
  can be constrained by th

Inclusive charge asymmet

- in agreement with NNLO
  predictions
- **4.7σ from no-asymmet**
- EFT limits based on the i

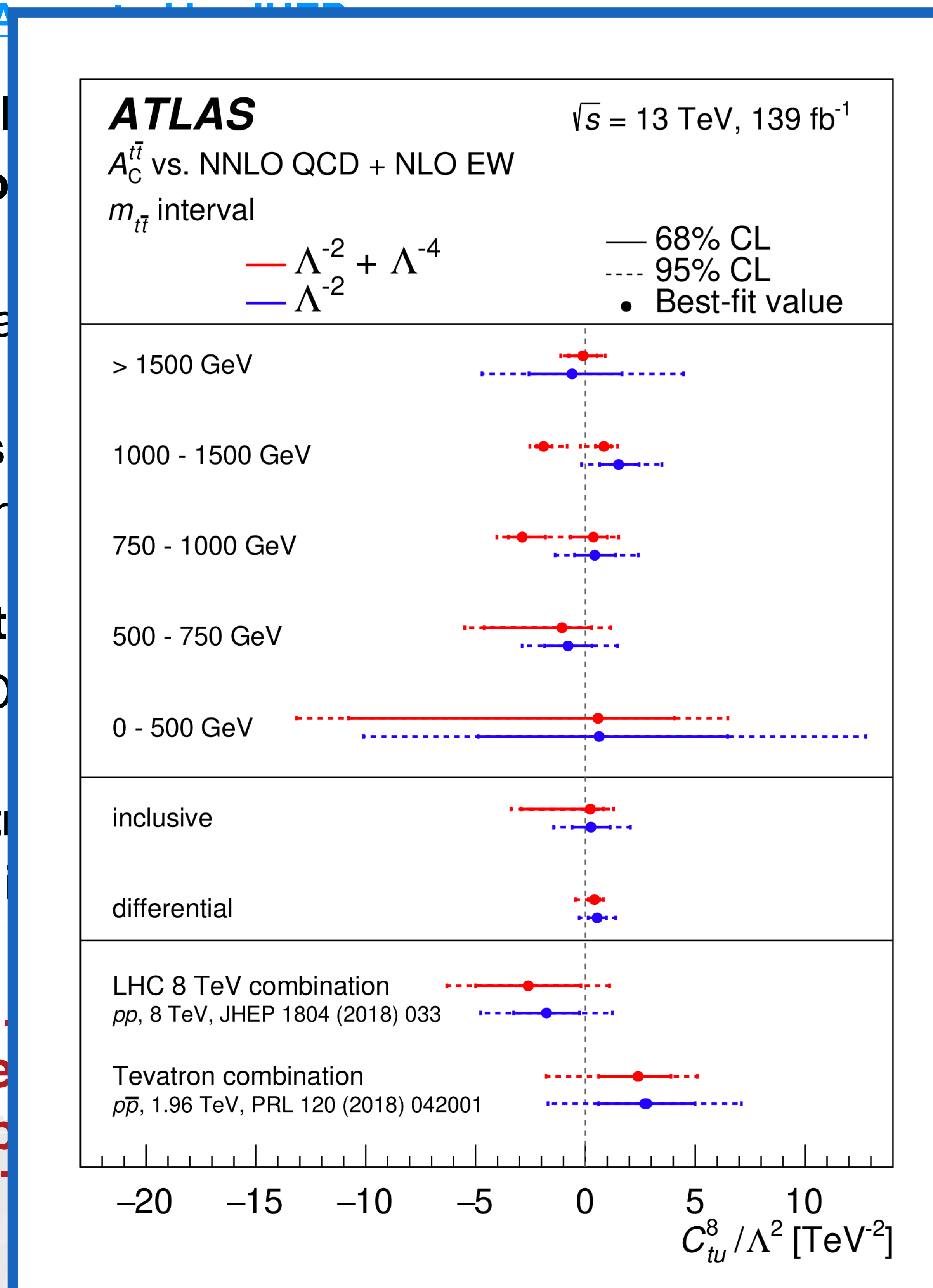

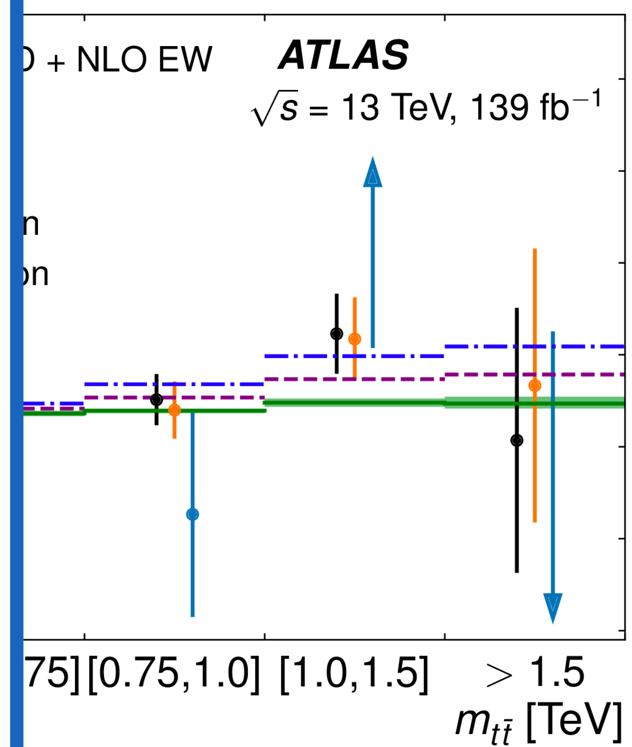

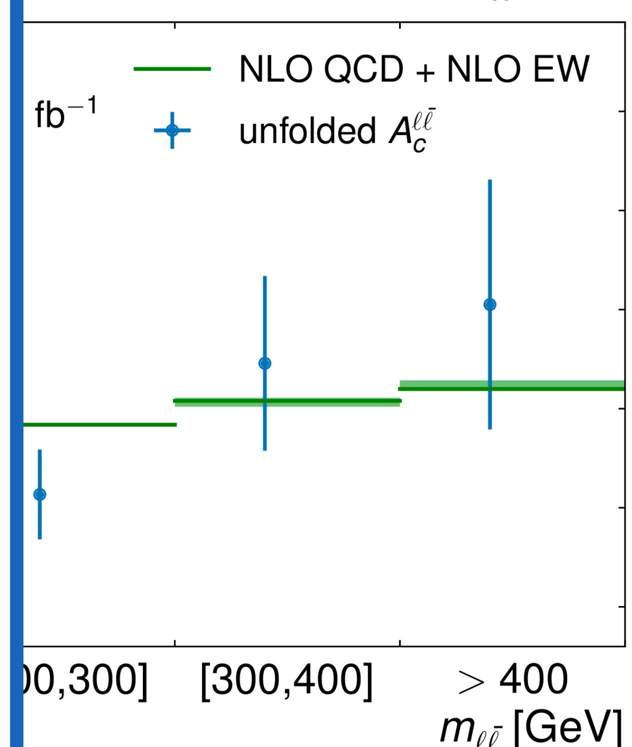

First evidence
asymmetry in p

$t\bar{t}$ charge asymmetry (boosted)

arXiv:2208.02751 - Submitted to PLB

New CMS measurement of A_C in l+jets boosted events ($m_{t\bar{t}}$ >750 GeV)

- in boosted environment qg or qq productions are enhanced → larger A_C
- top quarks produced with large Lorentz boosts →
  - non isolated leptons, unlike previous CMS results
  - overlapping jets
- three hadronic top categories: **resolved**, **semi-resolved** and **boosted**

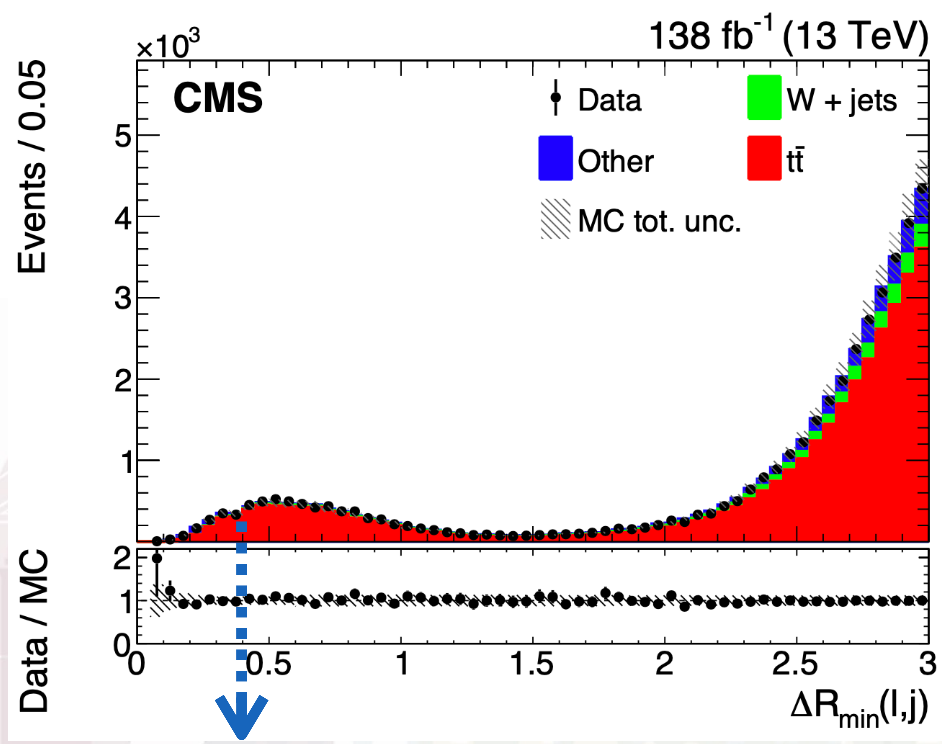

partially overlapping

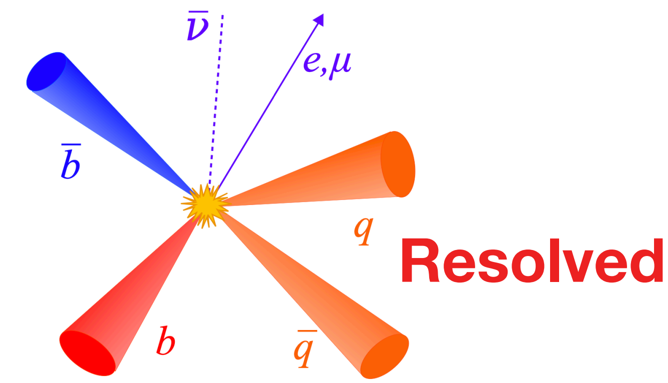

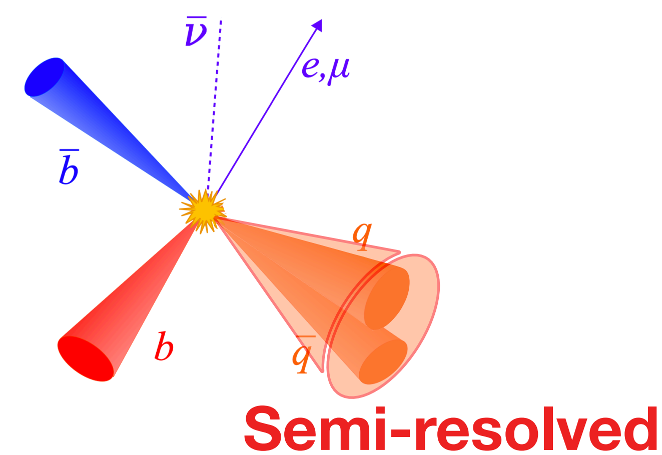

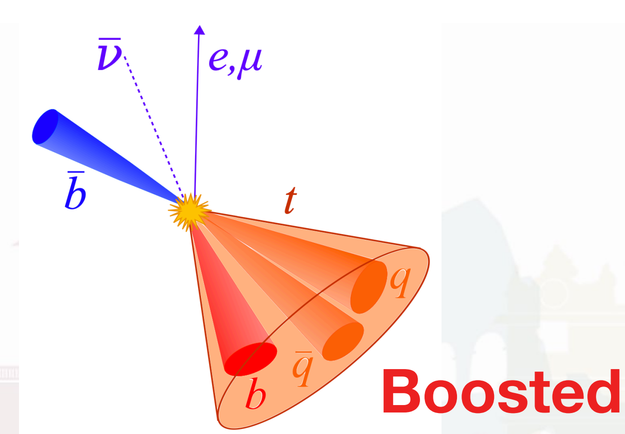

$t\bar{t}$ charge asymmetry (boosted)

arXiv:2208.02751 - Submitted to PLB

Data unfolded with a binned maximum likelihood fit and compared to theoretical prediction with NNLO QCD and NLO EW corrections

- $A_C^{\text{meas}} = (0.69^{+0.65}_{-0.69})\ \%$ (error is dominated by the statistical component)
- results are in very good agreement with the SM prediction

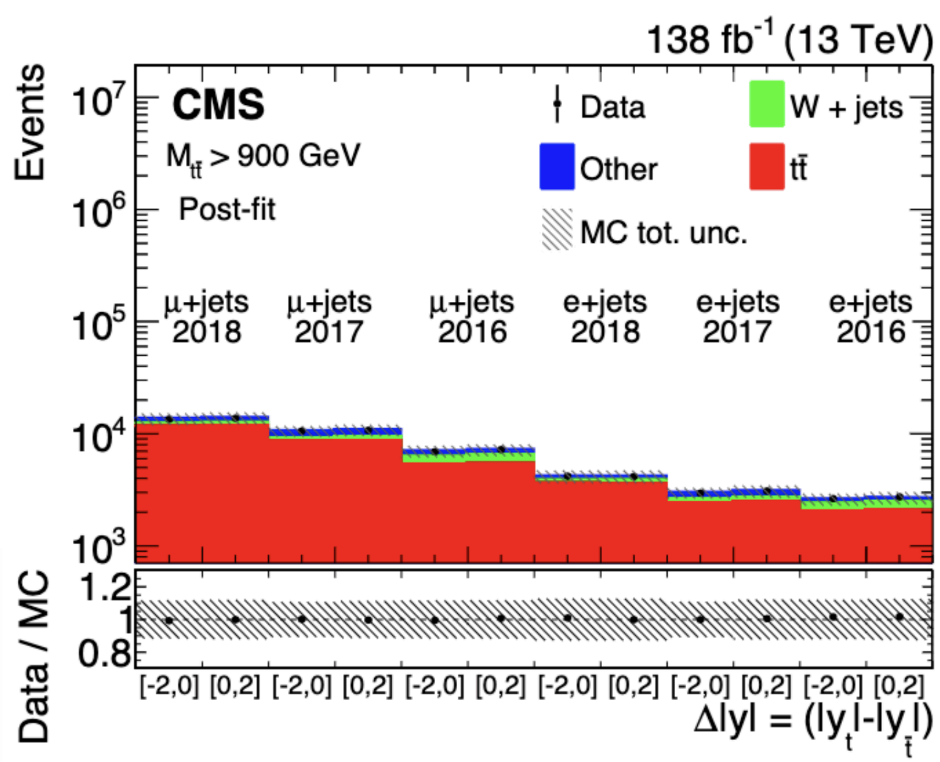

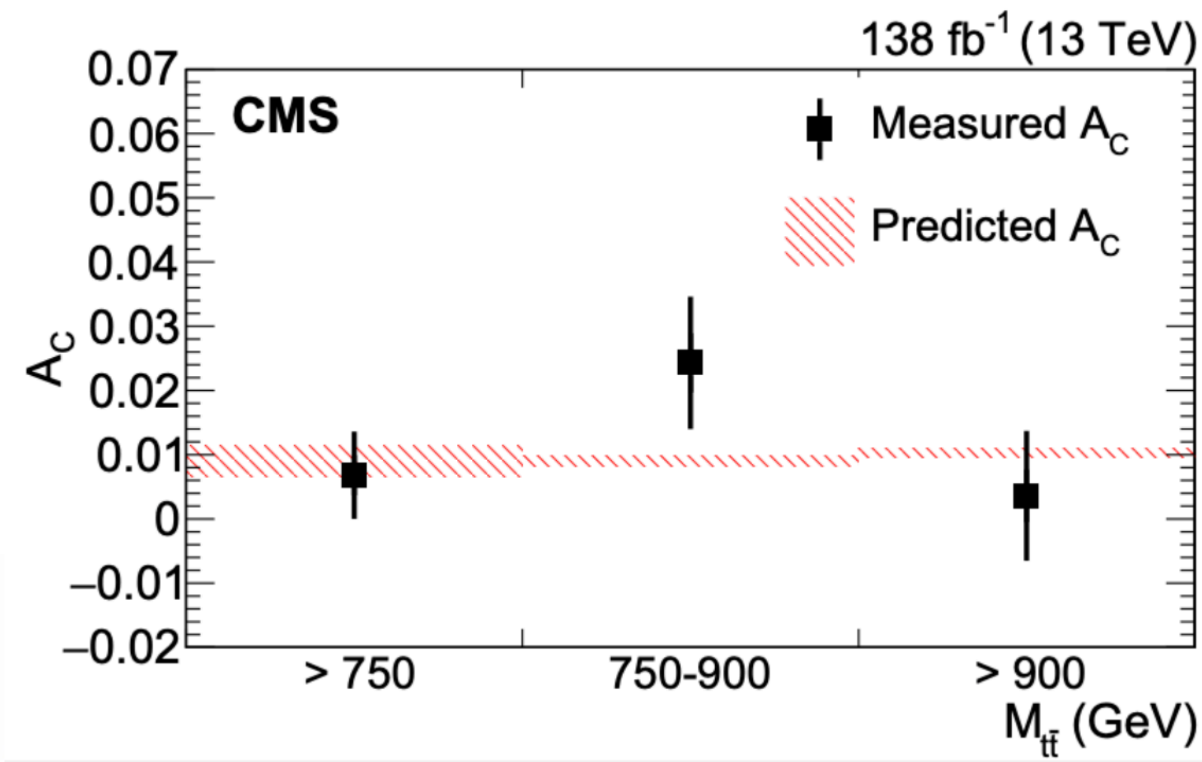

First charge asymmetry result in boosted regime

$t\bar{t}$+W charge asymmetry

arXiv:2301.04245

In $t\bar{t}$W production, the $q\bar{q}$' initial state leads to larger A_C than in $t\bar{t}$ production

- the W in $t\bar{t}$W is radiated from initial $q\bar{q}$' state and acts as event polarization, enhancing the asymmetry between the $t\bar{t}$

First measurement of A_C in $t\bar{t}$W using 139 /fb of ATLAS data at 13 TeV

- performed in the 3 charged leptons (e or μ) channel (3L)
- signal and control regions (SRs and CRs) defined by requirements on number of jets and b-tagged jets
- dedicated CRs to estimate the non-prompt lepton source from HF/LF decay or ɣ-conv.
- BDT trained to achieve the best “lepton–top-quark” association (71% efficient)

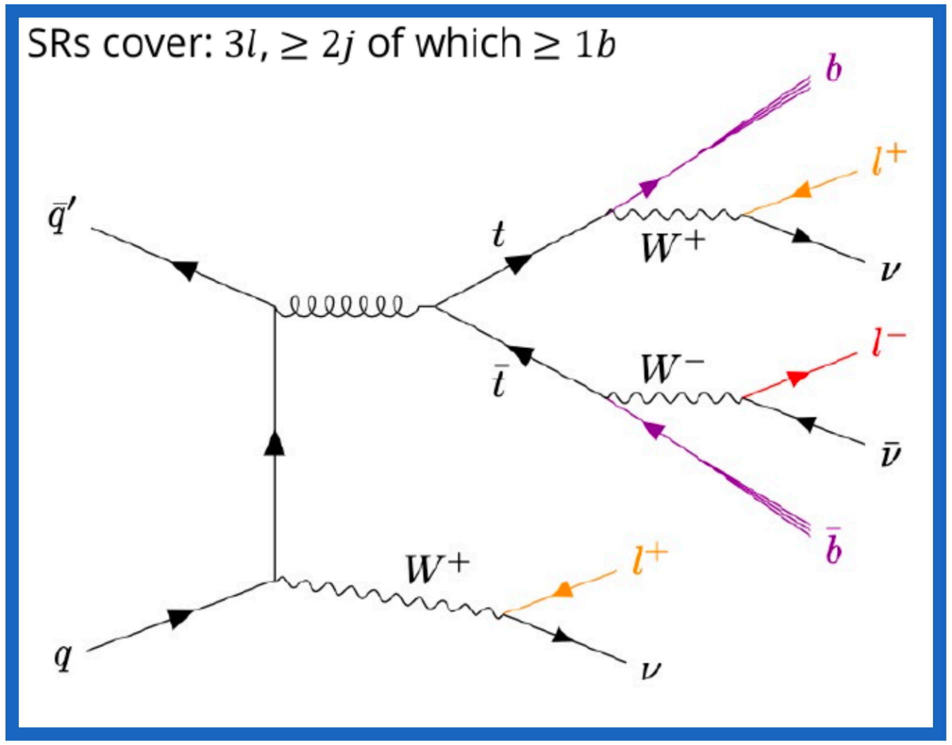

Odd lepton: always from (anti)top quark
Even leptons: need to select the correct one

$t\bar{t}$+W charge asymmetry

arXiv:2301.04245

Simultaneous fit to the numbers of observed events in the SRs

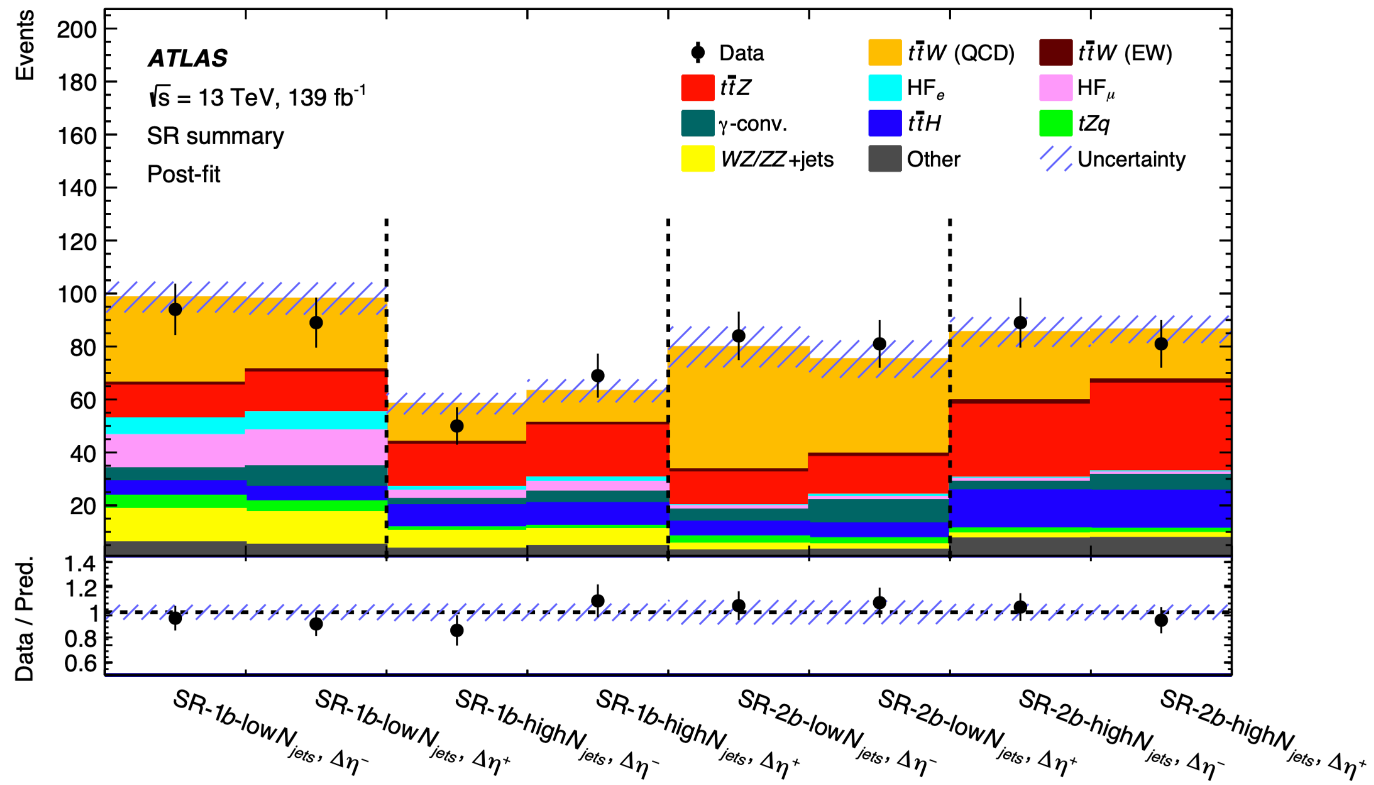

At reconstruction level:

- $A_C^{\ell\ell} = (-12.3 \pm 13.6\,(\text{stat.}) \pm 5.1\,(\text{syst.}))\,\%$

  $A_{C\,SM}^{\ell\ell} = (-8.4^{+0.5}_{-0.3}(\text{scale}) \pm 0.6(\text{MC stat.}))\,\%$ from SHERPA

After unfolding at particle level and fiducial phase space:

- $A_C^{\ell\ell} = (-11.2 \pm 17.0\,(\text{stat.}) \pm 5.5\,(\text{syst.}))\,\%$

  $(A_{C\,SM}^{\ell\ell} = (-6.3^{+0.7}_{-0.4}(\text{scale}) \pm 0.4(\text{MC stat.}))\,\%$ from SHERPA

Statistically dominated. In agreement with SM predictions

Overview of $t\bar{t}$(+X) asymmetries

ATL-PHYS-PUB-2023-013

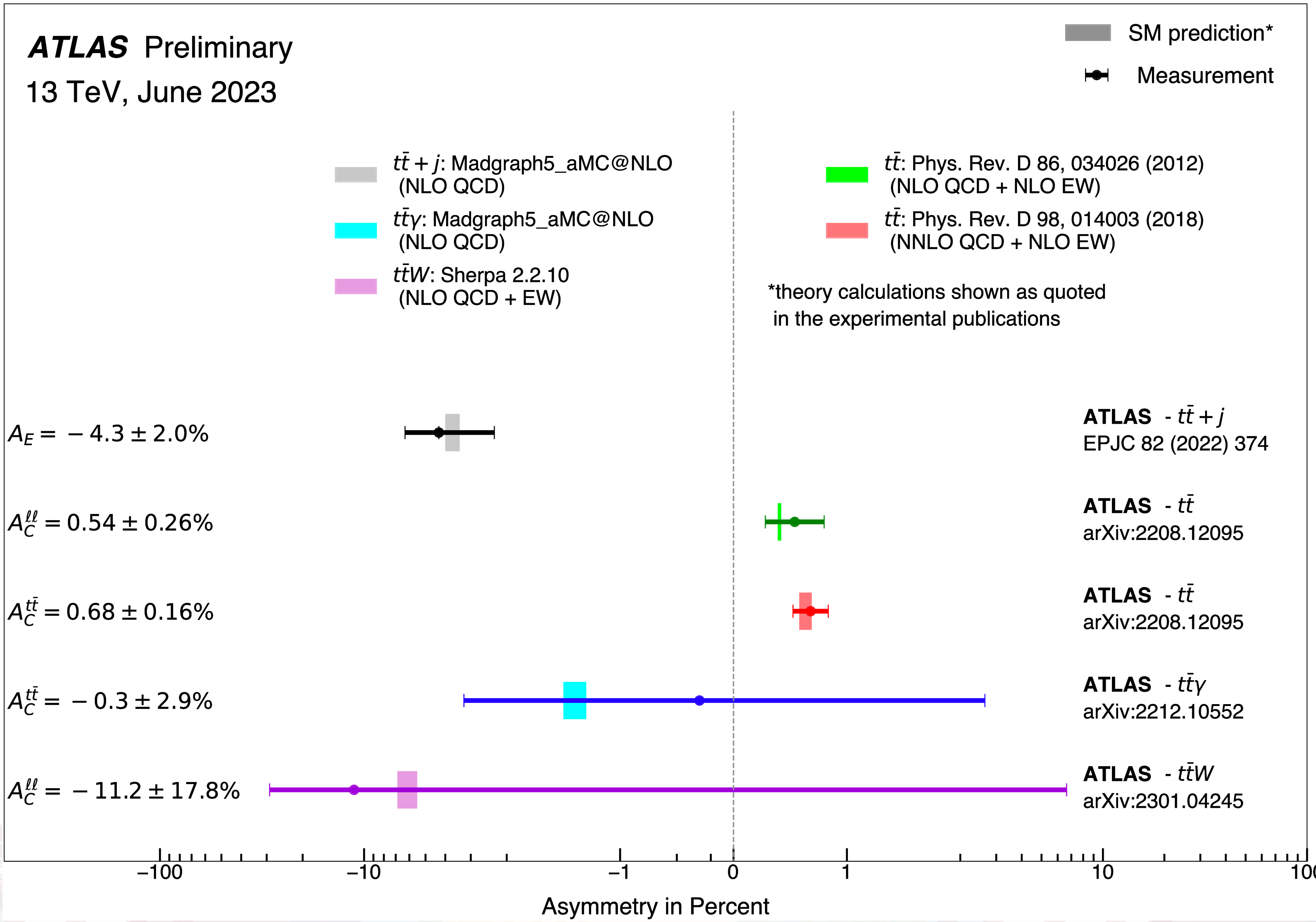

All asymmetries in good agreement with the most precise SM calculations

$t\bar{t}$ spin correlation

[Phys. Rev. D 100 (2019) 072002](#)

In $t\bar{t}$ production, top quarks produced unpolarised because of QCD parity conservation

- → correlated spins between top pairs
- accessible via $|\Delta\phi_{\ell\ell}|$, in dilepton $t\bar{t}$ decays, no top reconstruction required

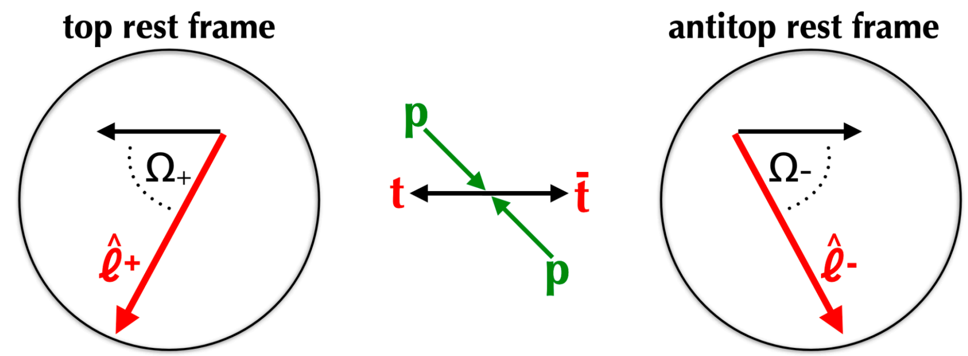

$$\frac{1}{\sigma}\frac{d\sigma}{d\Omega_+ d\Omega_-} = \frac{1}{(4\pi)^2}\left(1 + \mathbf{B}^+ \cdot \hat{\ell}^+ + \mathbf{B}^- \cdot \hat{\ell}^- - \hat{\ell}^+ \cdot \mathbb{C} \cdot \hat{\ell}^-\right)$$

Most recent CMS measurement of top-quark polarisation and $t\bar{t}$ spin correlation in dilepton events at 13 TeV

- Relative lepton directions follow 3x3 matrix C of spin correlation coefficients
- 15 coefficients ($B_i^{\pm}$,C_{ij}) characterize spin dependence of production
- each coefficient probed by measuring 1D angular distribution at parton level
- spin decorrelation D measured indirectly by $\frac{1}{\sigma}\frac{d\sigma}{d\cos\phi_{\ell\ell}} = \frac{1}{2}(1 - D\cos\phi_{\ell\ell})$

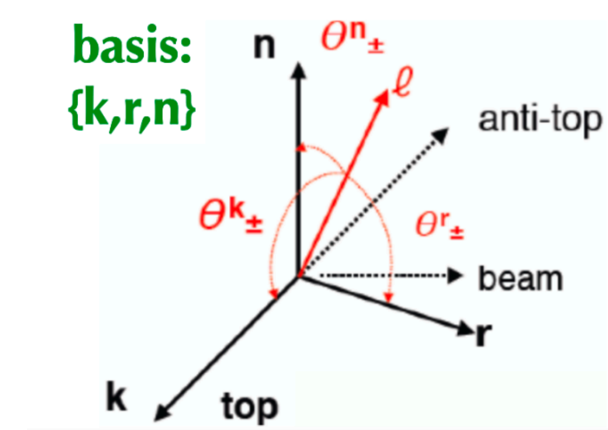

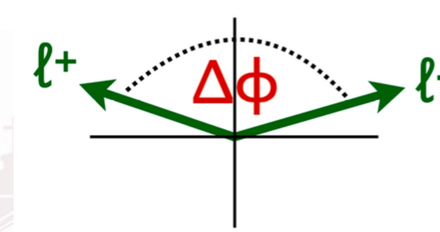

$t\bar{t}$ spin correlation

[Phys. Rev. D 100 (2019) 072002](#)

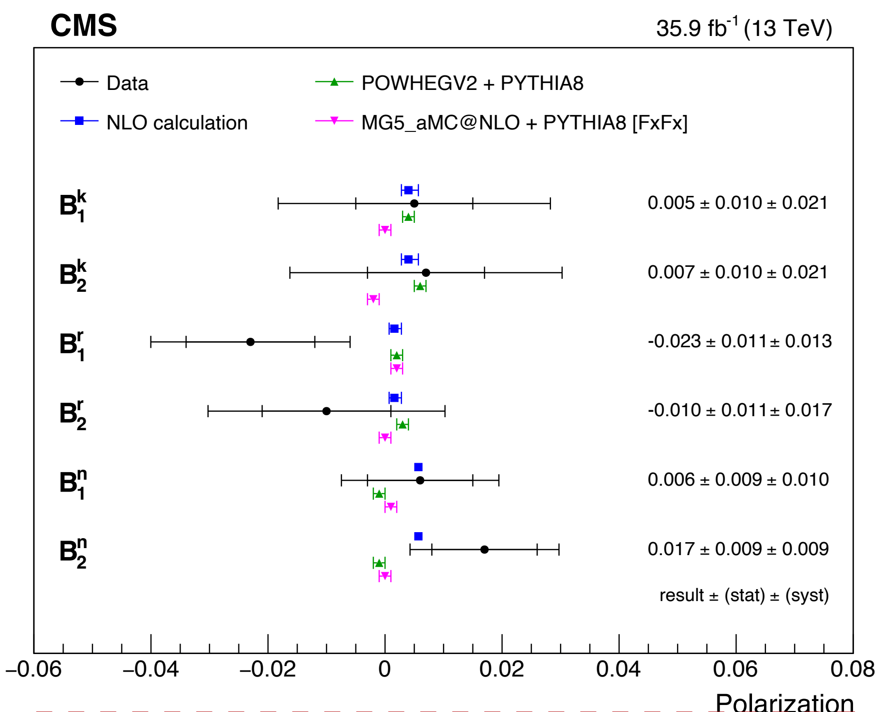

Top quark polarization (six B coefficients) consistent with zero

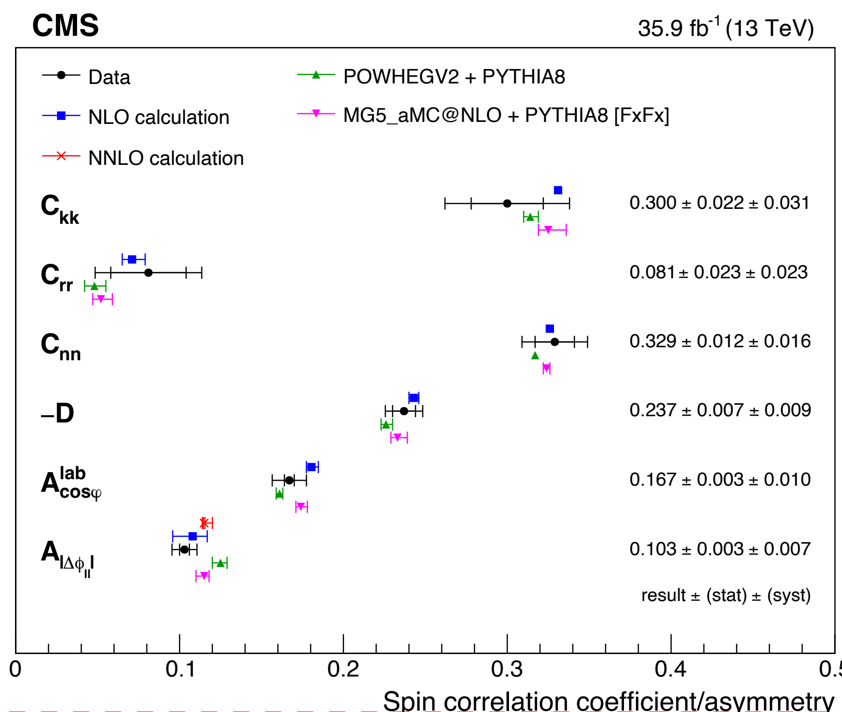

Spin diagonal coefficients (C_{ii}) consistent with expectations

Observations are consistent with the SM predictions

Results used to set constraints on top quark chromomagnetic, chromoelectric dipole moments (CMDM and CEDM) and anomalous couplings

- CMDM: $-0.24 < C_{tG}/\Lambda^2 < 0.07$ TeV^{-2} @ 95% C.L
- CEDM: $-0.33 < C^I_{tG}/\Lambda^2 < 0.20$ TeV^{-2} @ 95% C.L.

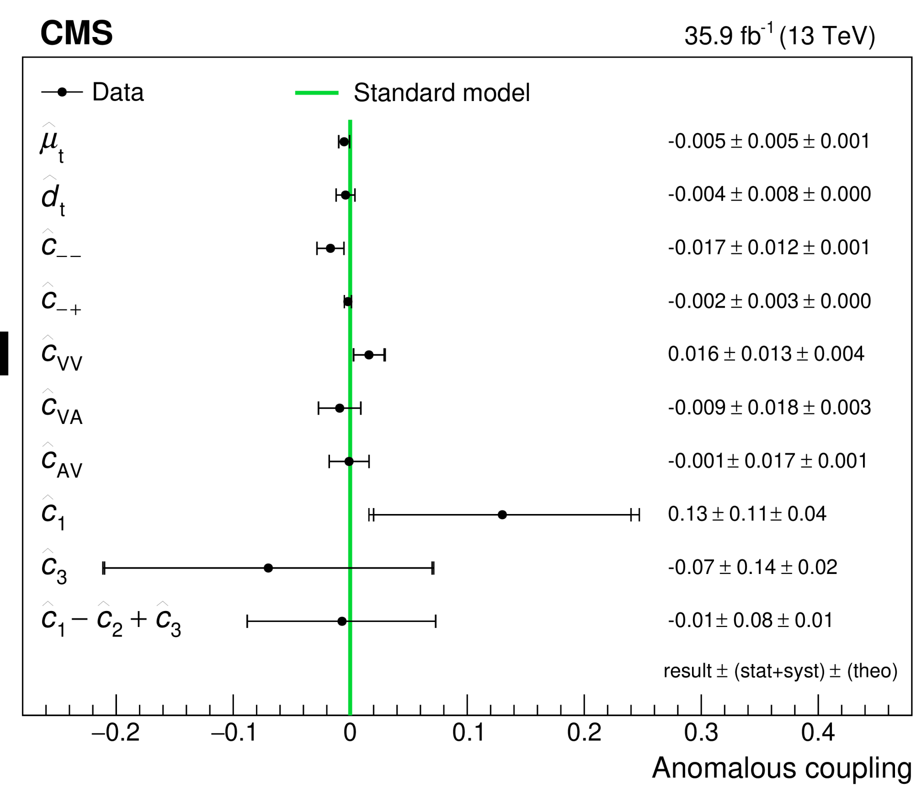

W helicity

Phys. Lett. B 843 (2023) 137829

Wtb properties in $t\bar{t}$ events determined by structure of weak interaction

- W bosons polarised mostly longitudinally (F_0) or left-handed (F_L) in the SM ($F_0 + F_L + F_R = 1$)
- sensitive to anomalous Wtb couplings (any significant F_R = new physics!)

longitudinal W **L-handed W** **R-handed W**

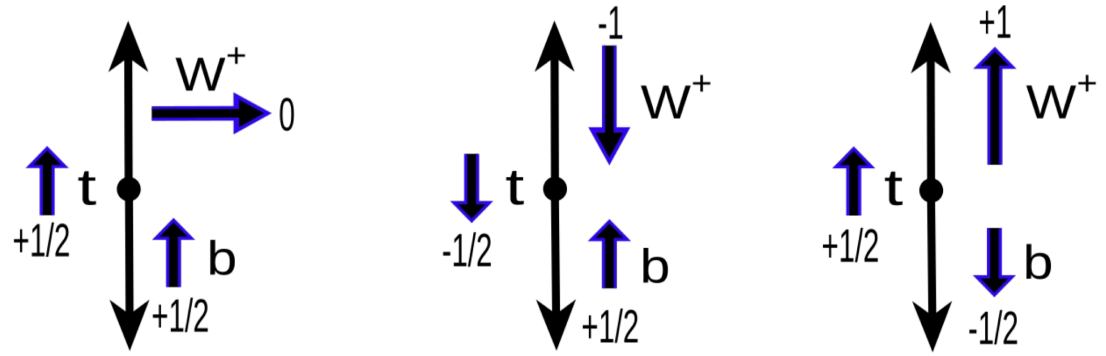

→ $F_L = 0.311 \pm 0.005$

$F_0 = 0.687 \pm 0.005$

$F_R = 0.0017 \pm 0.0001$

Measurement performed using 139 /fb of ATLAS data at 13 TeV

- opposite-sign dilepton channel extremely pure in $t\bar{t}$ events (>97%)
- Neutrino Weighting (NW) algorithm to remove events with poorly reconstructed kinematics

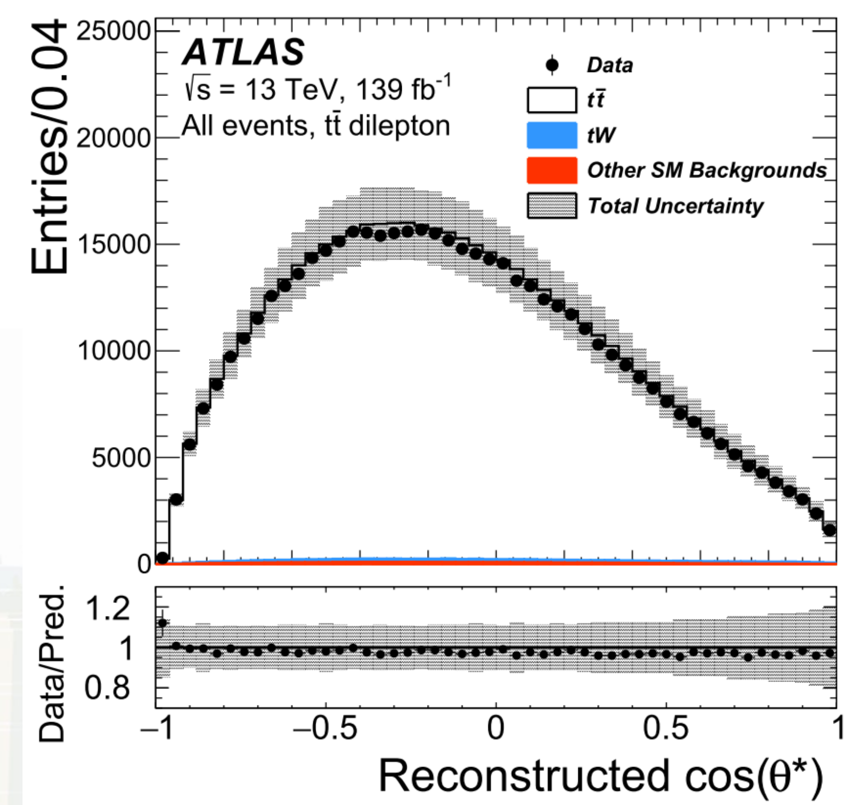

W helicity

[Phys. Lett. B 843 (2023) 137829]

The differential decay rate of top quarks considering the angle θ* is given by

- normalized angular distribution of charged lepton decay from the W unfolded to particle level using an iterative Bayesian unfolding (IBU) method

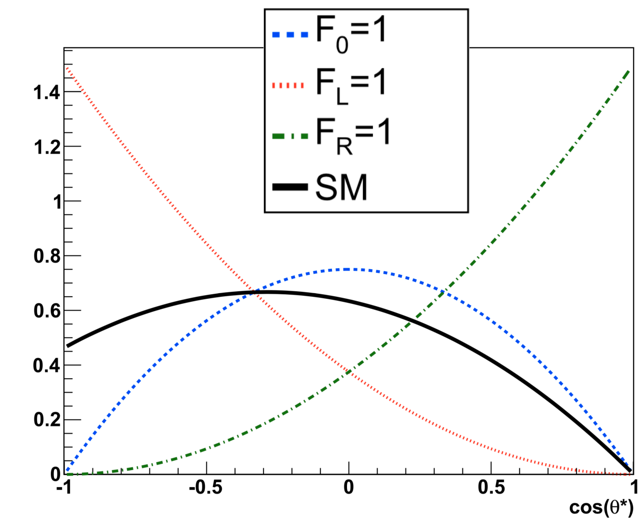

$$\frac{1}{\sigma}\frac{d\sigma}{d\cos\theta^*} = \frac{3}{4}\left(1-\cos^2\theta^*\right) F_0 + \frac{3}{8}\left(1-\cos\theta^*\right)^2 F_L + \frac{3}{8}\left(1+\cos\theta^*\right)^2 F_R$$

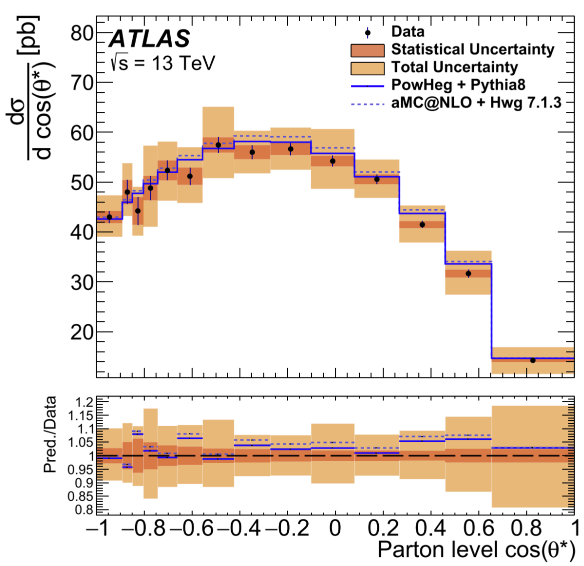

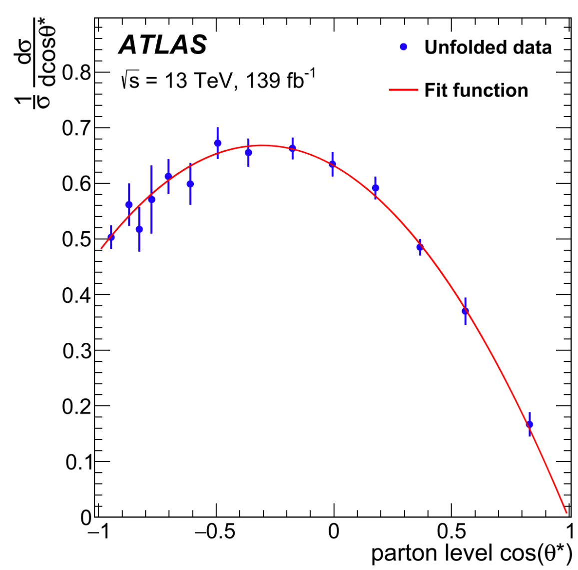

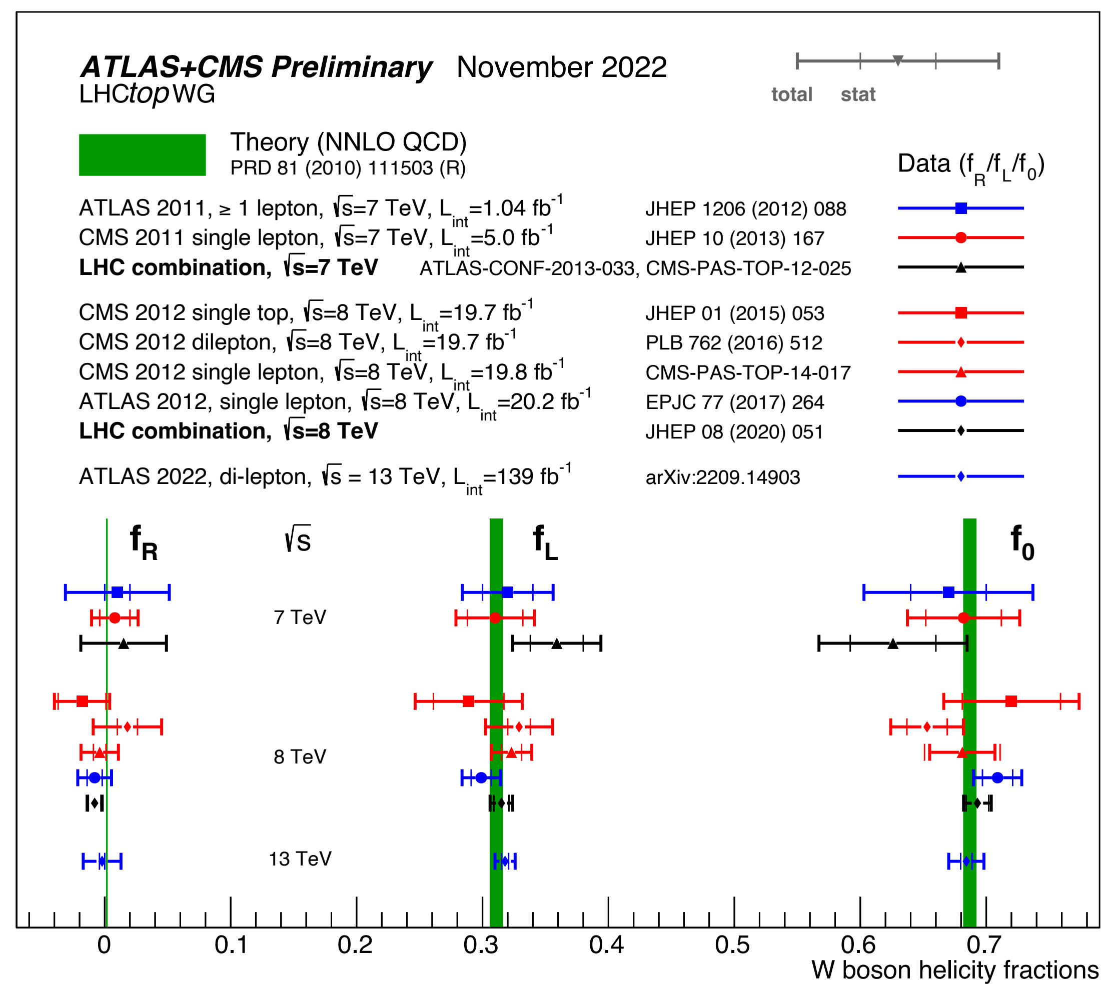

F_0 = 0.684 ± 0.005 (stat.) ± 0.014 (syst.)
F_L = 0.318 ± 0.003 (stat.) ± 0.008 (syst.)
F_R = –0.002 ± 0.002 (stat.) ± 0.014 (syst.)

In agreement with SM calculation at NNLO(QCD)

Top-quark polarisation

JHEP11 (2022) 040

At the LHC (pp collisions)...

- *EW production:* highly polarised top quarks due to V-A nature
- *detectable:* accessible via angular distributions (in top rest frame)
- *spin polarisation:* depends upon specific top-/antitop- sample and chosen basis

$$_{+}P_i = \frac{N(\uparrow) - N(\downarrow)}{N(\uparrow) + N(\downarrow)}, \quad \uparrow / \downarrow \text{ w.r.t. } i$$

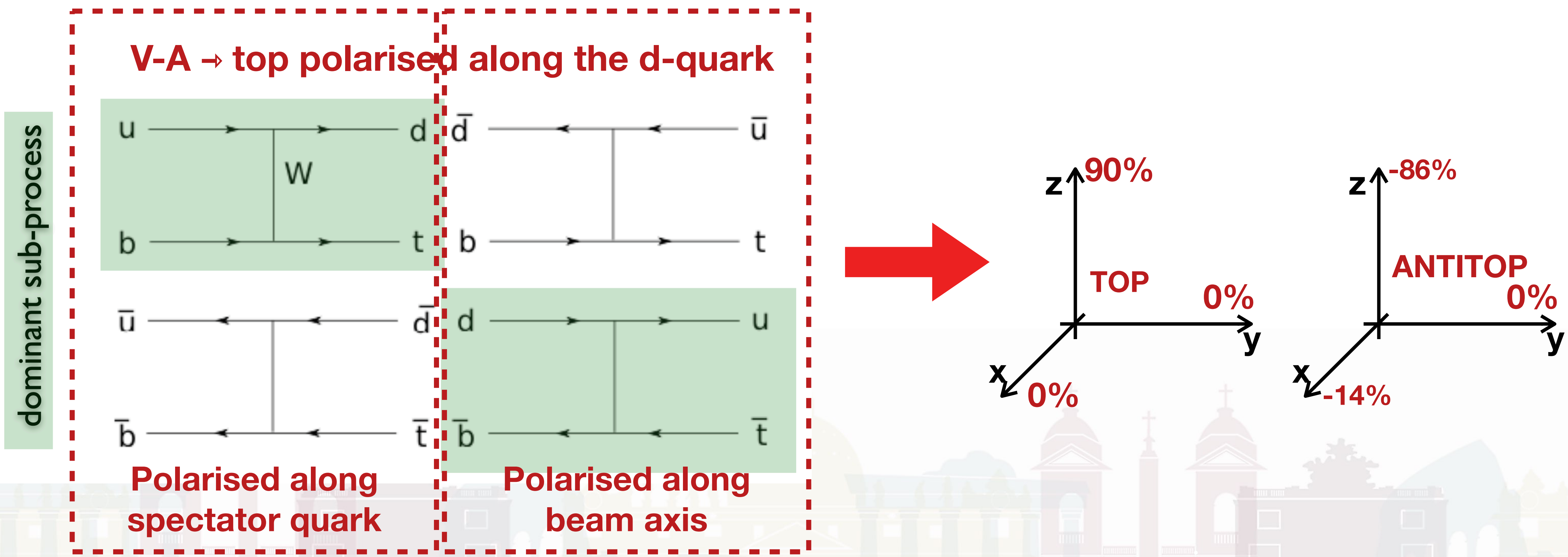

Top-quark polarisation

JHEP11 (2022) 040

Fiducial measurement of top polarisation in t-channel with full Run II dataset (139 /fb)

- *template fit:* measurement of top quark and anti-quark polarisations at reco. level within a fiducial region
- *unfolding:* normalised differential measurements ($\cos\theta_{x/y/z}$) unfolded at particle level
- *EFT interpretation* of the unfolded results

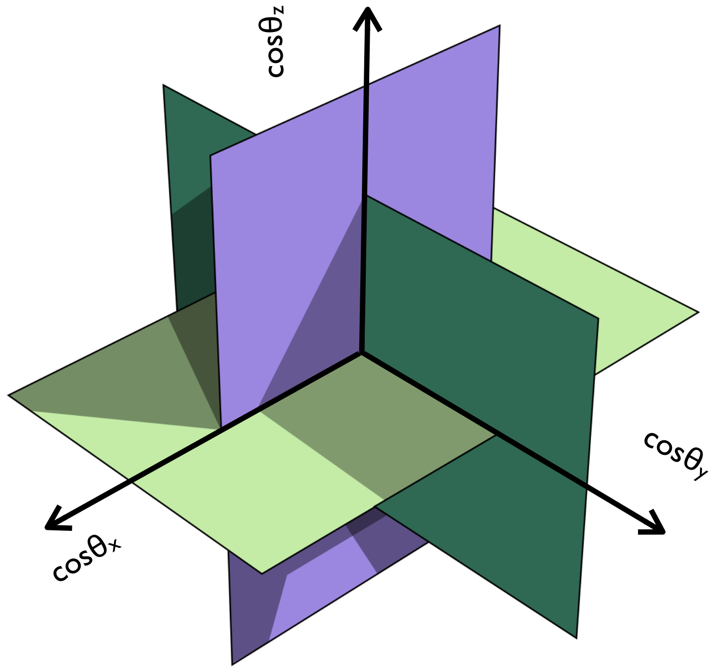

ℓ+jets channel and profile likelihood fit of polarisations:

- *4 regions:* 2 SRs (top, anti-top) + 2 CRs (W+jets, $t\bar{t}$)
- *6 polarisations* $P(t)=\{P_x^t, P_y^t, P_z^t\}$ and $P(\bar{t})=\{P_x^{\bar{t}}, P_y^{\bar{t}}, P_z^{\bar{t}}\}$
- *Octant distribution "Q"* to fit in SR (**$\cos\theta_x$** / **$\cos\theta_y$** / **$\cos\theta_z$**)

Top-quark polarisation

JHEP11 (2022) 040

ATLAS EXPERIMENT

Fiducial measurement of top polarisation in t-channel with full Run II dataset (139 /fb)

- *template fit:* measurement of top quark and anti-quark polarisations at reco. level within a fiducial region
- *unfolding:* normalised differential measurements ($\cos\theta_{x/y/z}$) unfolded at particle level
- *EFT interpretation* of the unfolded results

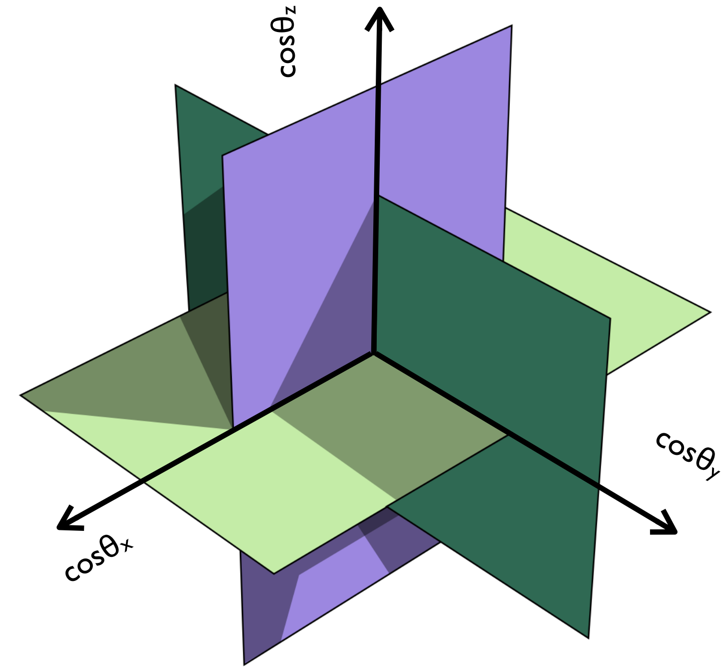

ℓ+jets channel and profile likelihood fit of polarisations:

Parameter	Extracted value	(stat.)
t-channel norm.	$+1.045 \pm 0.022$	(± 0.006)
$W+$jets norm.	$+1.148 \pm 0.027$	(± 0.005)
$t\bar{t}$ norm.	$+1.005 \pm 0.016$	(± 0.004)
$P^{t}_{x'}$	$+0.01 \pm 0.18$	(± 0.02)
$P^{\bar{t}}_{x'}$	-0.02 ± 0.20	(± 0.03)
$P^{t}_{y'}$	-0.029 ± 0.027	(± 0.011)
$P^{\bar{t}}_{y'}$	-0.007 ± 0.051	(± 0.017)
$P^{t}_{z'}$	$+0.91 \pm 0.10$	(± 0.02)
$P^{\bar{t}}_{z'}$	-0.79 ± 0.16	(± 0.03)

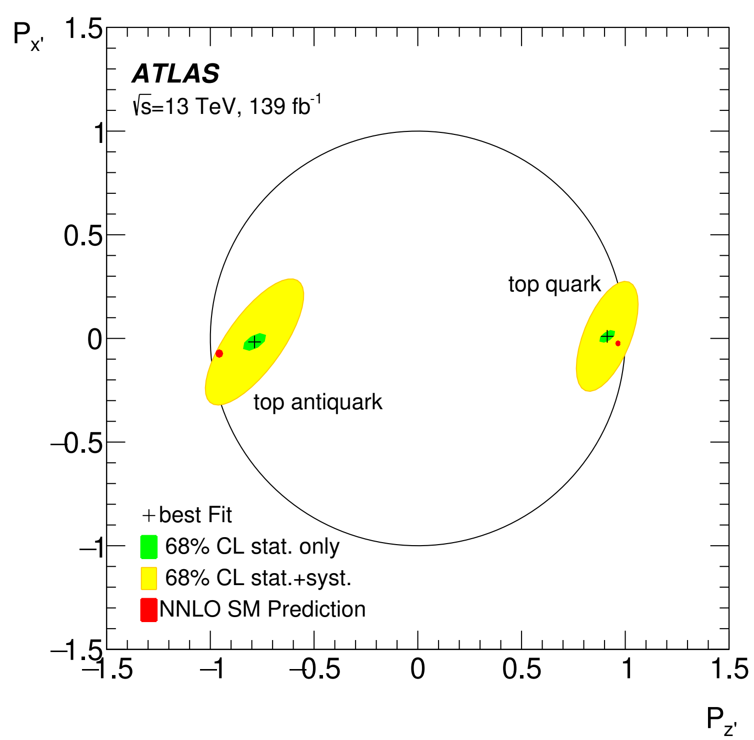

Very good agreement with NLO SM

Py ≈ 0 → no CP violation

Largest uncertainty from jet-energy resolution (JER)

Top-quark polarisation

JHEP11 (2022) 040

ATLAS EXPERIMENT

Three normalised angular observables ($\cos\theta_{x/y/z}$) unfolded to particle level

- Iterative Bayesian Unfolding (IBU) employed for deconvolution
- comparisons with different MC predictions at particle level in fiducial region

EFT interpretation of normalised $\cos\theta_{x/y}$ with morphing technique

- parametric description for EFT operators using minimal number of templates
- focus on O_{tW} (variables not sensitive to $O_{\phi Q}$, O_{qQ})

Sketch of a morphing example

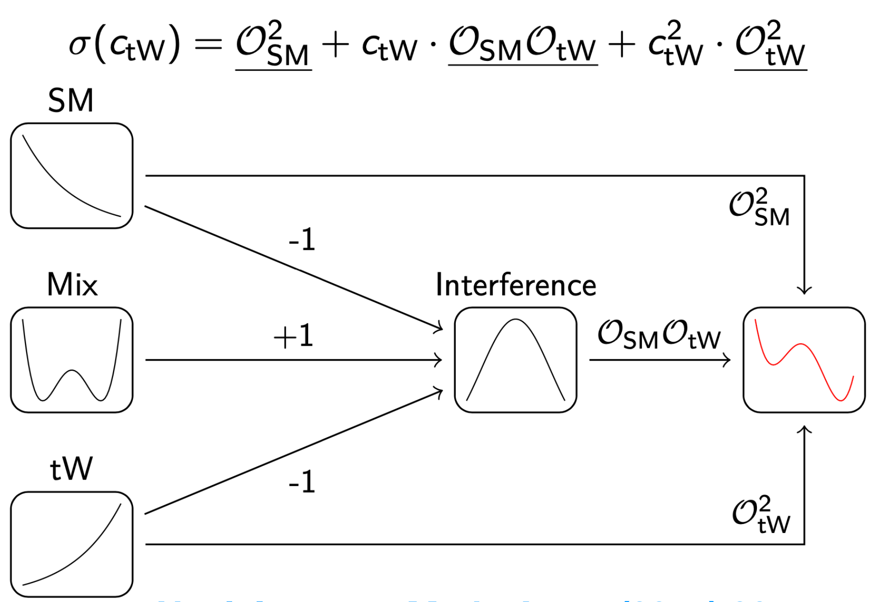

Nucl. Instrum. Meth. A 771 (2015) 39

	C_{tW}		C_{itW}	
	68% CL	95% CL	68% CL	95% CL
All terms	$[-0.3, 0.8]$	$[-0.9, 1.4]$	$[-0.5, -0.1]$	$[-0.8, 0.2]$
Order $1/\Lambda^4$	$[-0.3, 0.8]$	$[-0.9, 1.4]$	$[-0.5, -0.1]$	$[-0.8, 0.2]$
Order $1/\Lambda^2$	$[-0.3, 0.8]$	$[-0.8, 1.5]$	$[-0.6, -0.1]$	$[-0.8, 0.2]$

Top-quark polarisation

JHEP11 (2022) 040

ATLAS EXPERIMENT

Three normalised angular observables ($\cos\theta_{x/y/z}$) unfolded to particle level

- Iterative Bayesian Unfolding (IBU) employed for deconvolution
- comparisons with different MC predictions at particle level in fiducial region

EFT interpretation of normalised $\cos\theta_{x/y}$ with morphing technique

- parametric description for EFT operators using minimal number of templates
- focus on O_{tW} (variables not sensitive to $O_{\phi Q}$, O_{qQ})

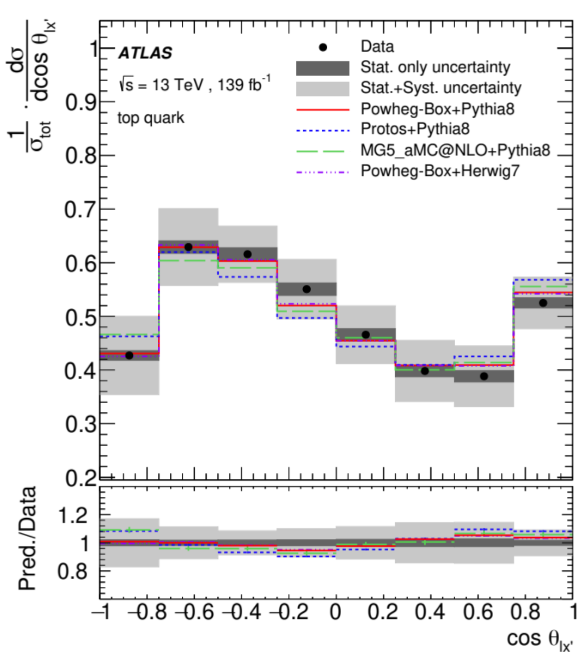

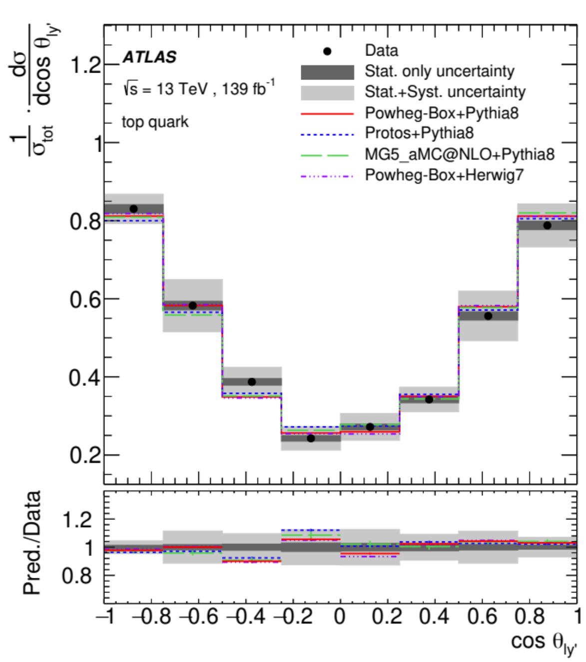

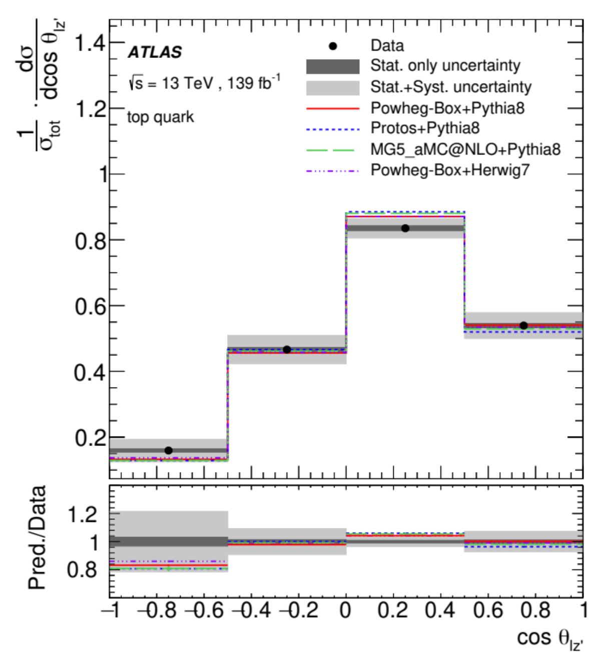

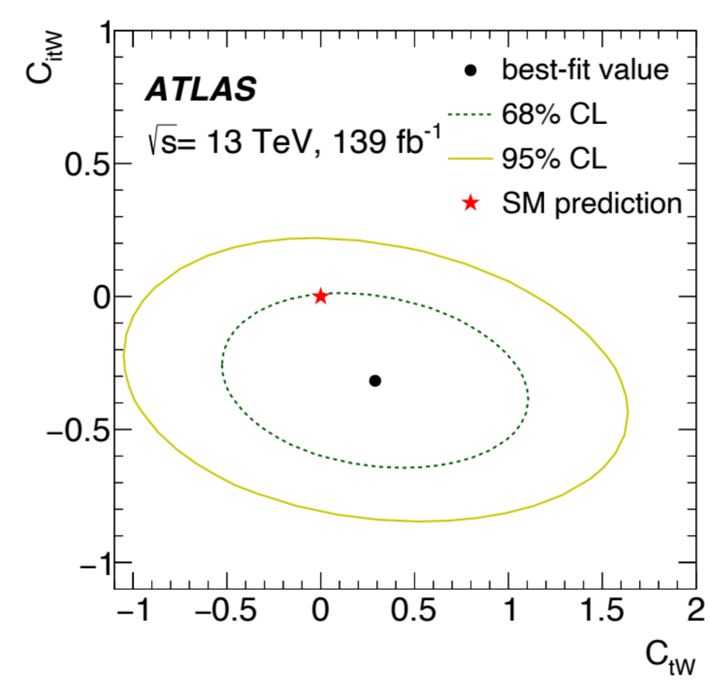

Very good agreement with NLO SM prediction

No deviation from 0 observed

Conclusion

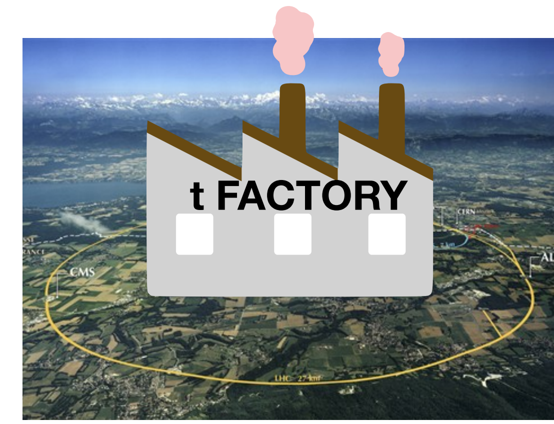

The top quark has come a long way since 1995 (discovery)

- back then: missing quark, similar to other quarks
- today: know that top quark is special

In precision era, top-quark spin is key to an abundance of different research areas

- so far, Standard Model describes data extremely well
- more results with the Run 2 dataset in the pipeline
- Run 3 (and beyond) promise even larger datasets

Many more exciting top physics results still to come!

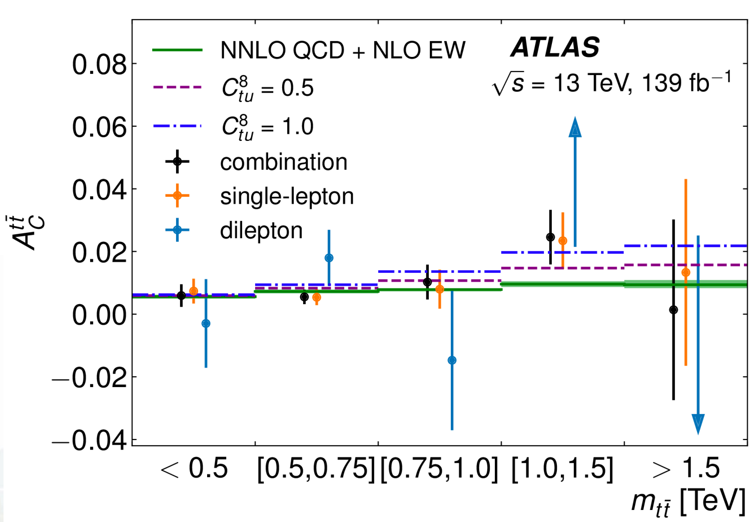

Evidence of charge asymmetry in pp collisions and first result in boosted regime!

Other charge asymmetry measurements in $t\bar{t}$+X

$t\bar{t}$ spin polarisations and correlation measurement

Most precise W helicity measurement so far

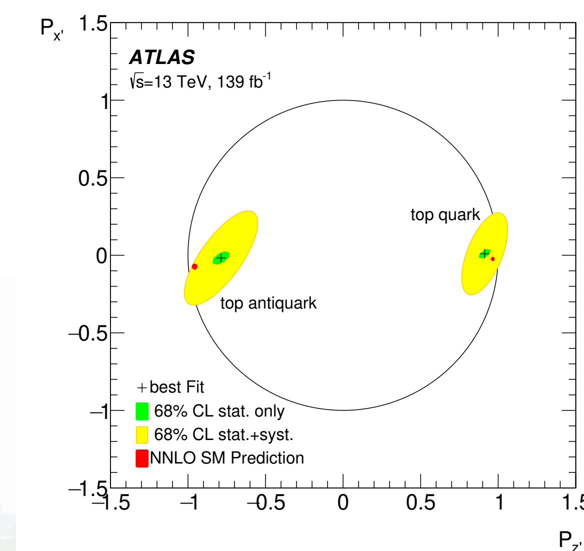

First top (anti-top) polarisation measurement at 13 TeV

Backup

Charge asymmetry

ATLAS-CONF-2019-026

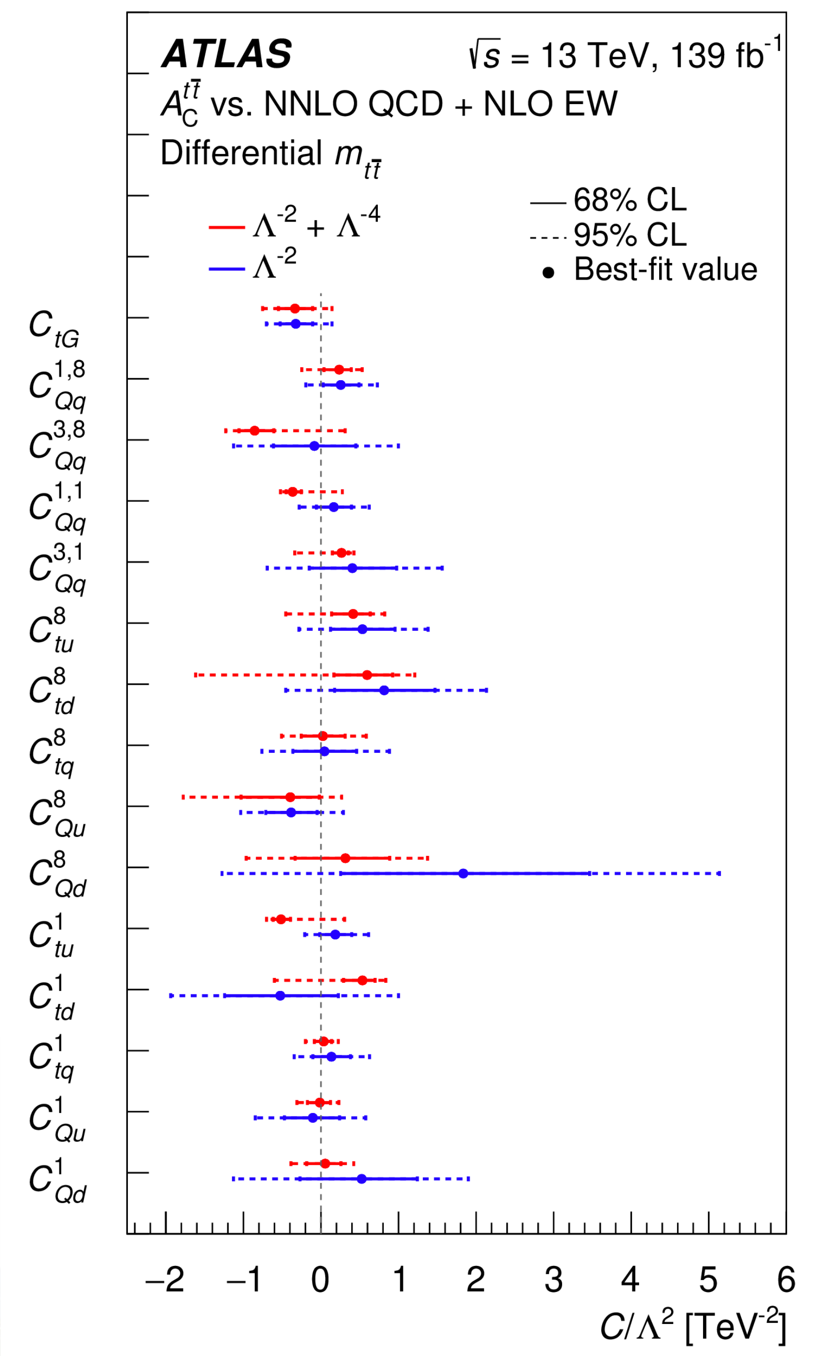

Measurements reinterpreted in EFT

- C^- = 4-fermion operator assuming flavour conservation and equal *u-d* type couplings (maps onto axi-gluon)
- theory paper: **JHEP03(2011)125**

Inclusive and differential results surpass ATLAS+CMS Run I combination

- no large dependence on quadratic terms
- dimension 6 approach is stable and appropriate

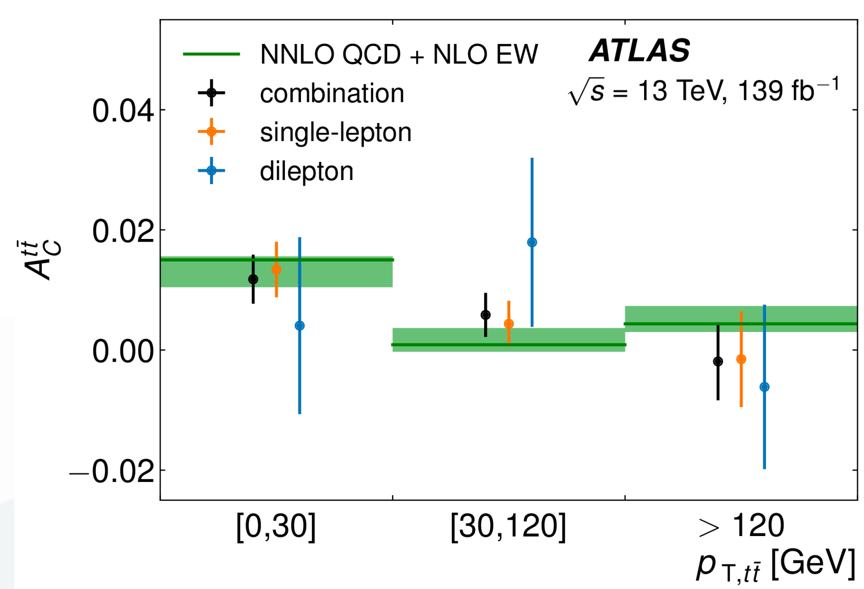

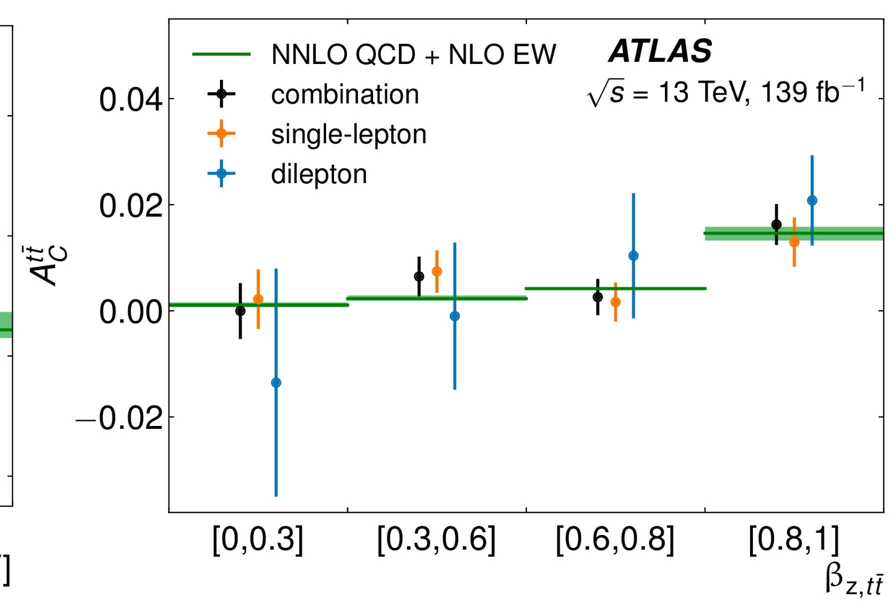

Charge asymmetry

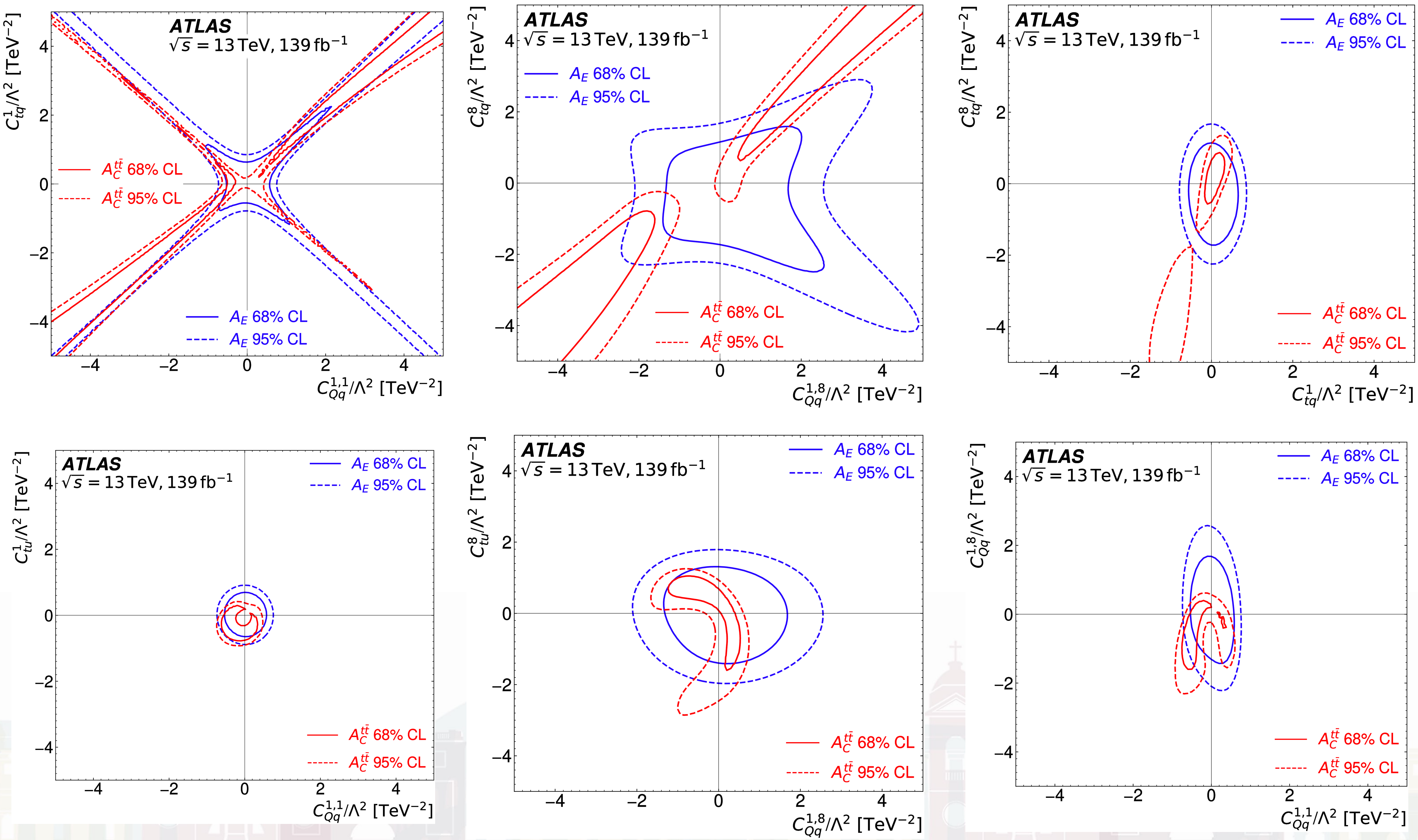

Charge asymmetry (boosted)

$M_{t\bar{t}}$ (GeV)	A_C (%) Measured	Stat	Syst	MC stat	Total	Theory
	Fiducial phase space (A_C^{fid})					
> 750	0.22	± 0.44	$^{+0.34}_{-0.43}$	± 0.32	$^{+0.64}_{-0.69}$	0.72 $^{+0.64}_{-0.61}$
750 – 900	0.39	$^{+0.66}_{-0.65}$	$^{+0.39}_{-0.56}$	$^{+0.43}_{-0.44}$	$^{+0.88}_{-0.96}$	0.60 $^{+0.97}_{-0.91}$
> 900	1.18	± 0.58	$^{+0.55}_{-0.75}$	± 0.41	$^{+0.90}_{-1.03}$	0.83 $^{+0.85}_{-0.82}$
	Full phase space (A_C)					
> 750	0.69	± 0.44	$^{+0.34}_{-0.42}$	± 0.32	$^{+0.65}_{-0.69}$	0.94 $^{+0.05}_{-0.07}$
750 – 900	2.43	± 0.65	$^{+0.29}_{-0.64}$	$^{+0.45}_{-0.43}$	$^{+0.84}_{-1.01}$	0.87 $^{+0.06}_{-0.08}$
> 900	0.37	± 0.58	$^{+0.55}_{-0.72}$	$^{+0.41}_{-0.40}$	$^{+0.90}_{-1.01}$	1.01 $^{+0.06}_{-0.07}$

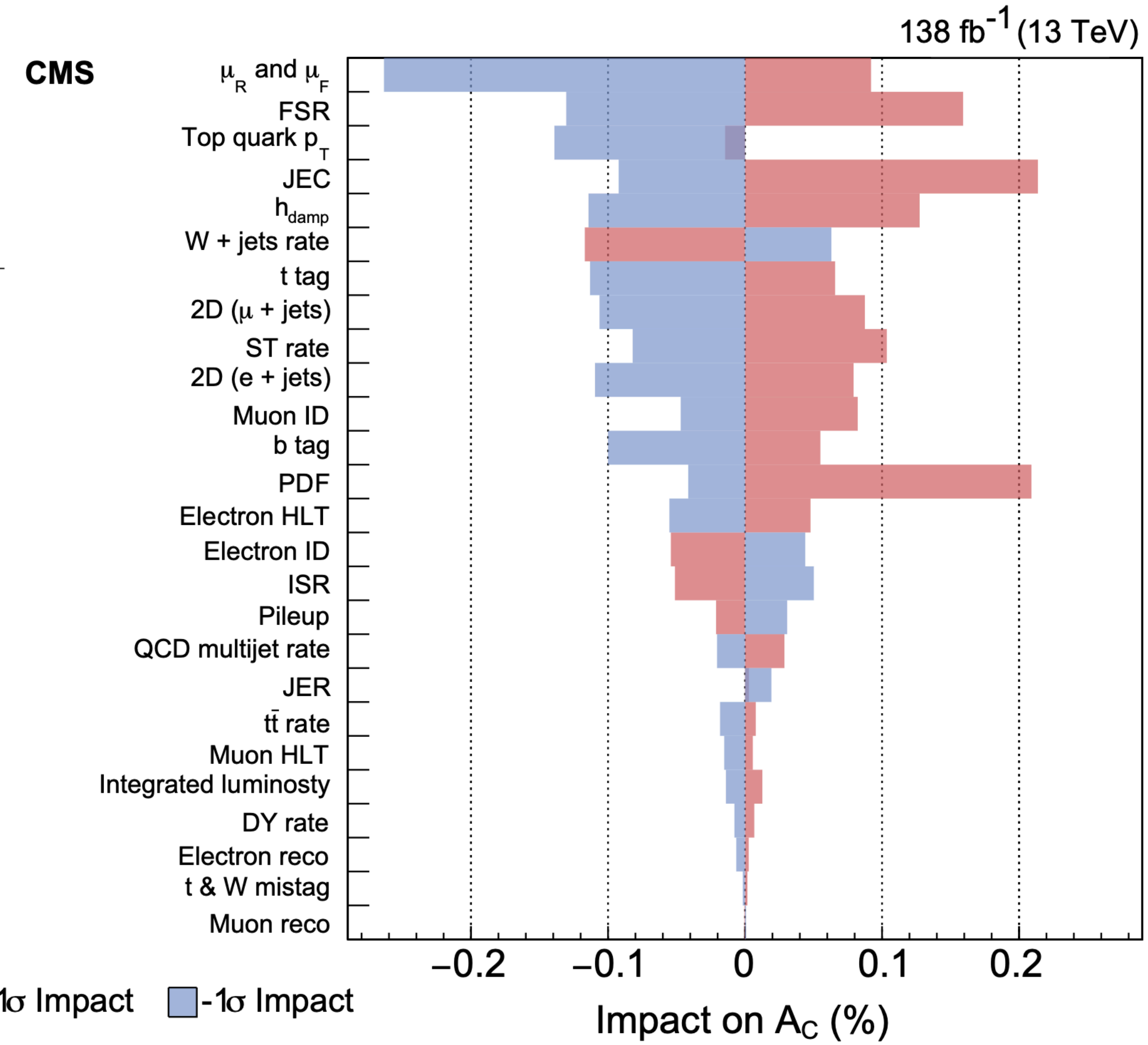

$t\bar{t}+\gamma$ charge asymmetry

[Phys. Lett. B 843 (2023) 137848]

$t\bar{t}+\gamma$ has enhanced $q\bar{q}$ initiated production

→ perfect playground for tests of $A_C^{t\bar{t}}$

- enhancement only for events where the photon is radiated by initial state partons (a.k.a. "$t\bar{t}+\gamma$ production")

$t\bar{t}+\gamma$ production

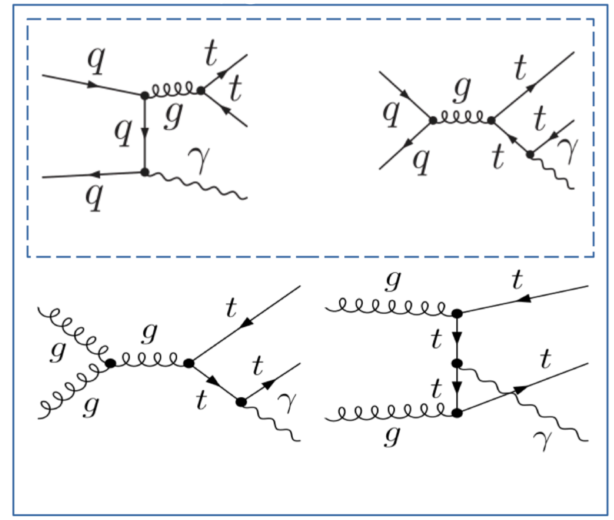

$t\bar{t}+\gamma$ decay

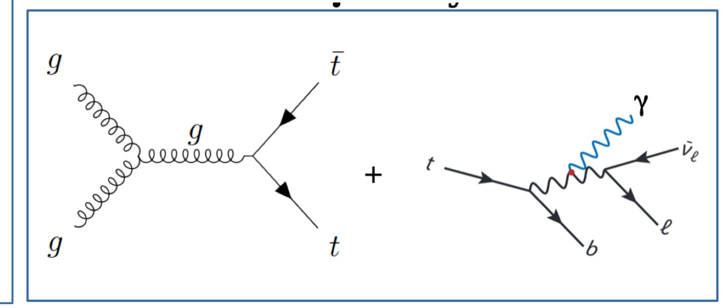

l+γ+jets selection with Run II data:

- kinematic likelihood fit (KLFitter) to reconstruct $t\bar{t}$ system
- Neural Network to separate signal ($t\bar{t}+\gamma$ prod) vs. backgrounds
  - "$t\bar{t}+\gamma$ decay" as irreducible background
  - two regions NN<0.6 and NN>0.6

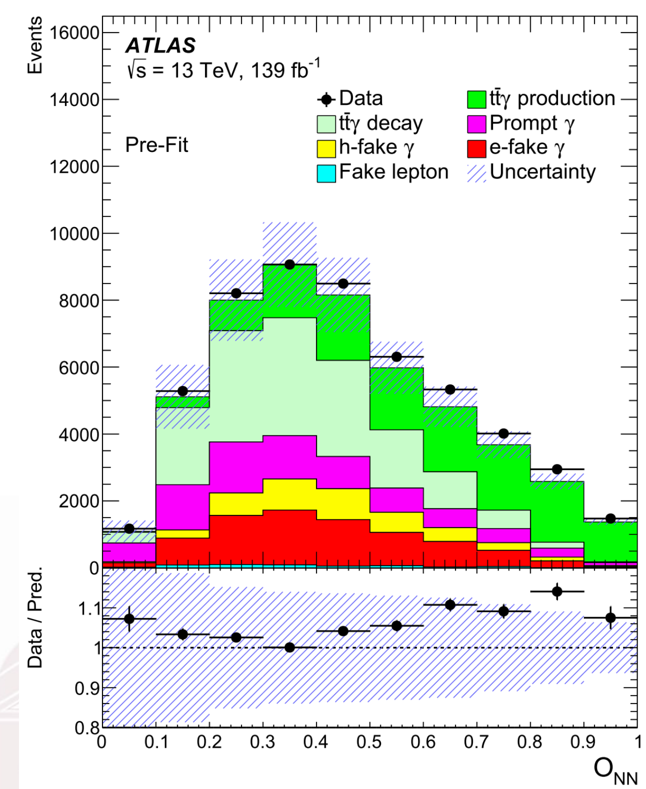

Main backgrounds: prompt γ, jet- and e-faking γ

- $t\bar{t}+\gamma$ decay (30%) and prompt-γ (15%) estimated with MC
- data-driven e-faking γ (16%) using tag-and-probe Z→ee/eγ events
- data-driven jet-faking γ (7%) using ABCD method (γ-iso and γ-ID)

$t\bar{t}+\gamma$ charge asymmetry

[Phys. Lett. B 843 (2023) 137848]

$A_C^{t\bar{t}}$ extraction by Profile Likelihood Unfolding (PLU)

- $A_C^{t\bar{t}} = -0.003 \pm 0.029 = -0.003 \pm 0.024(\text{stat}) \pm 0.017(\text{syst})$
- precision is limited by the statistical uncertainty

Total uncertainty	0.029
Statistical uncertainty	0.024
MC statistical uncertainties	
Background processes	0.008
$t\bar{t}\gamma$ production	0.004
Modelling uncertainties	
$t\bar{t}\gamma$ production modelling	0.003
Background modelling	0.002
Prompt background normalisation	0.002
Experimental uncertainties	
Jet	0.009
Fake-lepton background estimate	0.005
E_T^{miss}	0.005
Fake-photon background estimates	0.003
Photon	0.001
b-tagging	0.001
Other experimental	0.004

Consistent with SM prediction
$A_C^{t\bar{t}} = -0.014 \pm 0.001$ (MadGraph NLO)

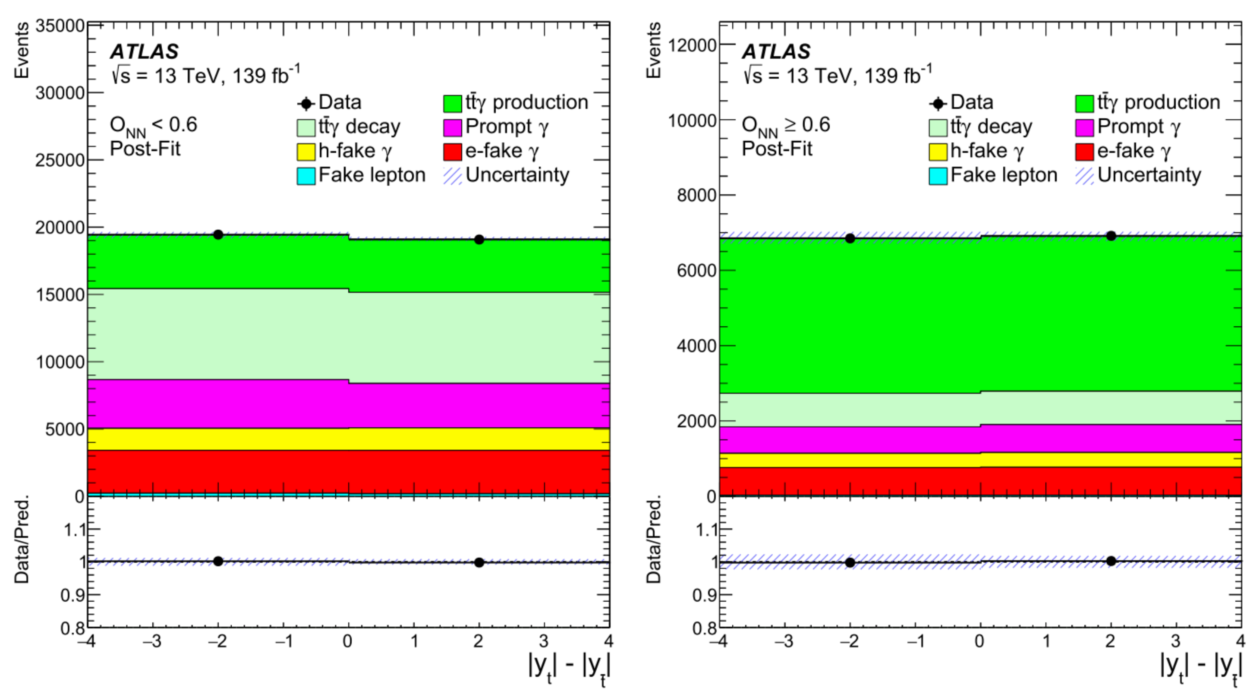

$t\bar{t}+\gamma$ charge asymmetry

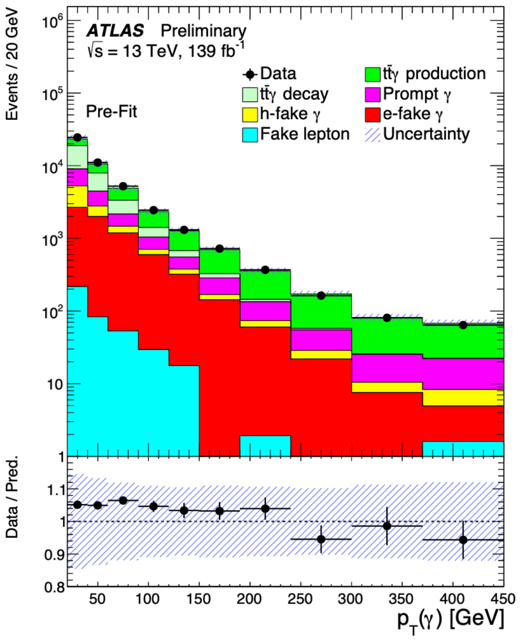

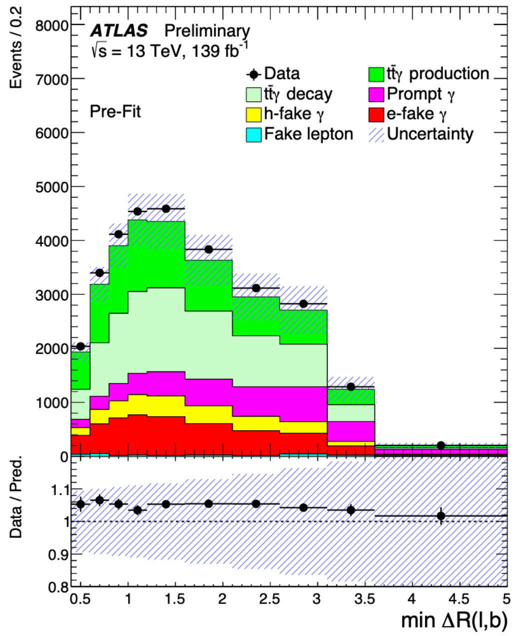

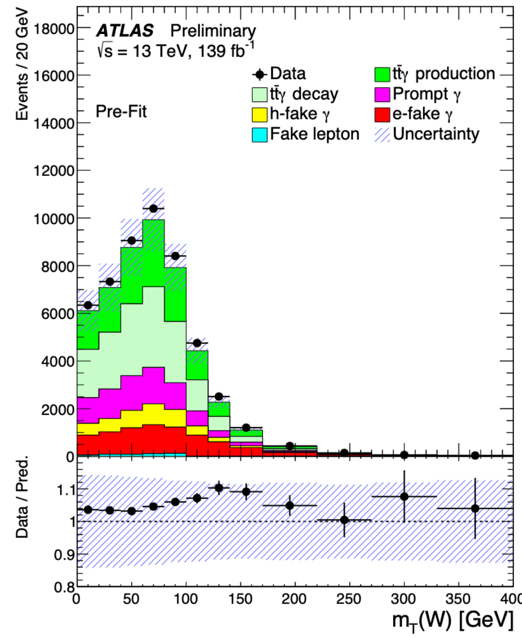

	$O_{NN} < 0.6$	$O_{NN} \geq 0.6$
$t\bar{t}\gamma$ prod (signal)	6660 ± 350	6910 ± 340
$t\bar{t}\gamma$ decay	14 100 ± 3100	1900 ± 560
h-fake γ	3400 ± 1400	790 ± 360
e-fake γ	6420 ± 860	1480 ± 260
prompt γ	6400 ± 2000	1300 ± 400
lepton fake	410 ± 110	57 ± 35
Total	37 400 ± 4500	12 400 ± 1100
Data	38527	13763

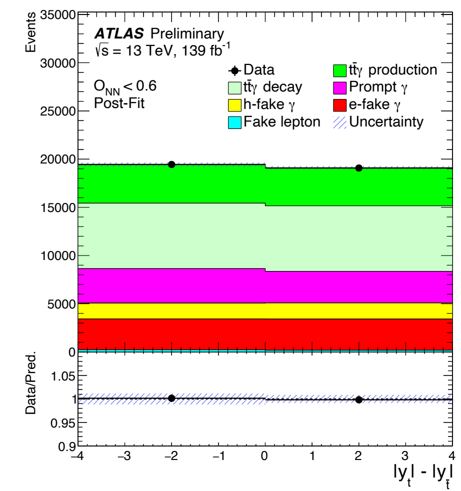

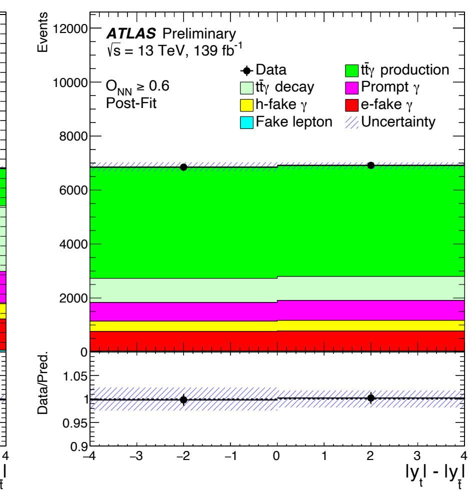

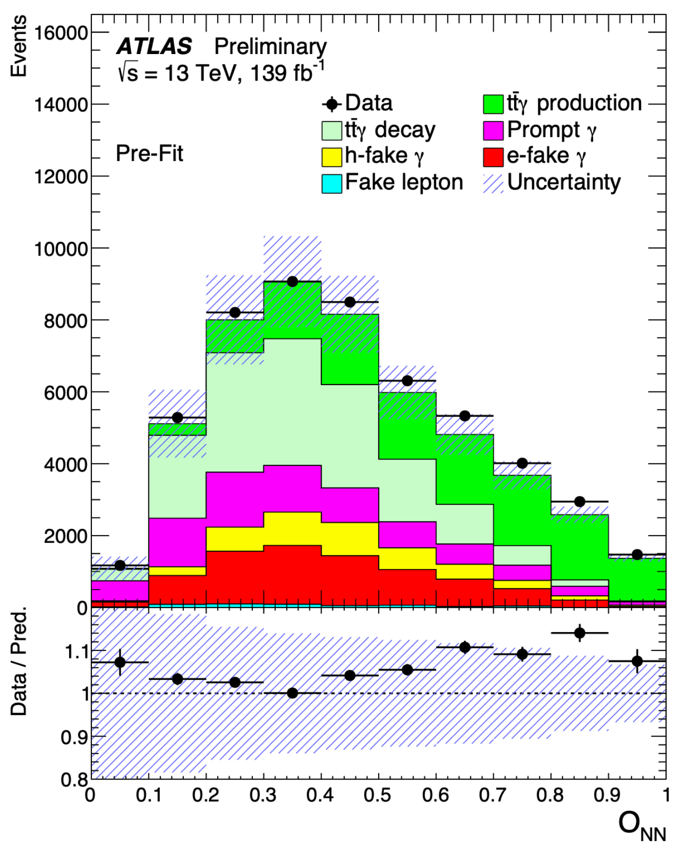

Total uncertainty	0.030
Statistical uncertainty	0.024
MC statistical uncertainties	
$t\bar{t}\gamma$ production	0.004
Background processes	0.008
Modelling uncertainties	
$t\bar{t}\gamma$ production modelling	0.003
Background modelling	0.002
Prompt background normalisation	0.003
Experimental uncertainties	
Jet and b-tagging	0.010
Fake lepton background estimate	0.005
$E_{\mathrm{T}}^{\mathrm{miss}}$	0.009
Fake photon background estimates	0.004
Photon	0.003
Other experimental	0.004

tt̄W charge asymmetry

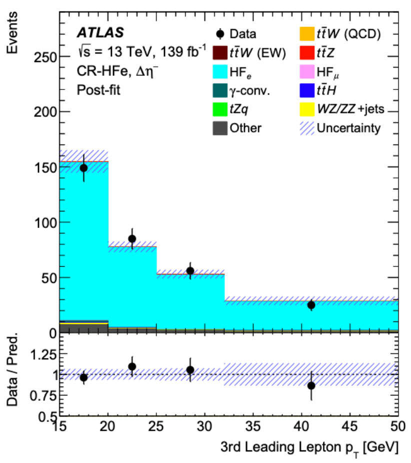

(a)

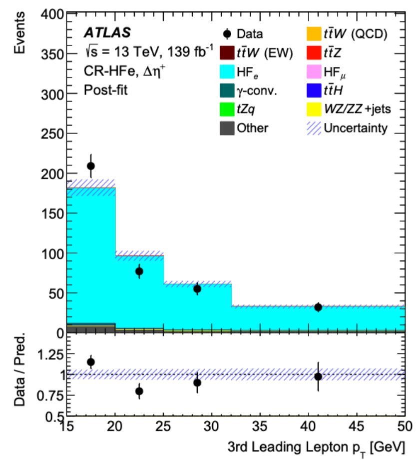

(b)

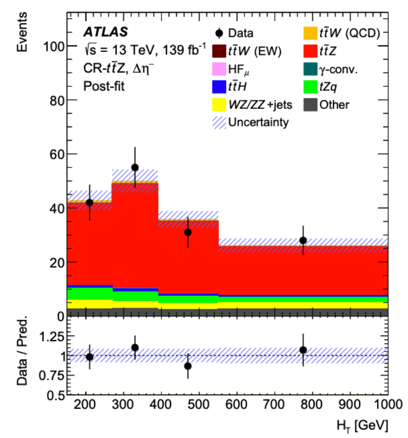

(a)

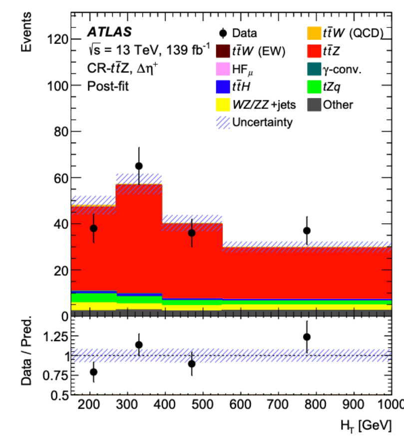

(b)

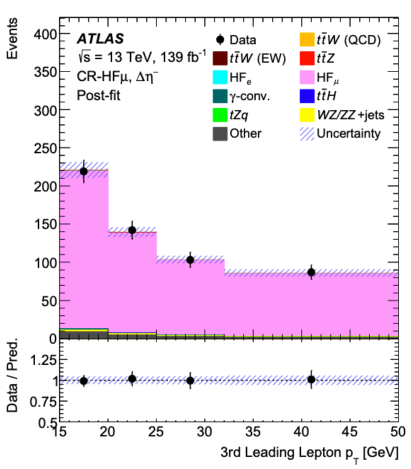

(c)

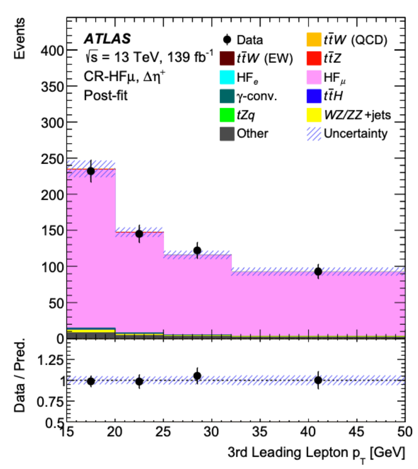

(d)

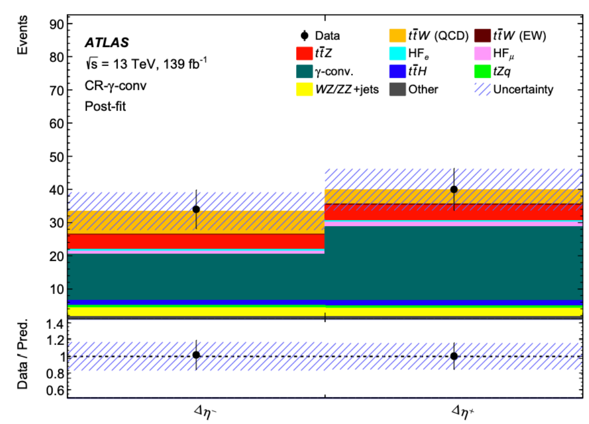

(c)

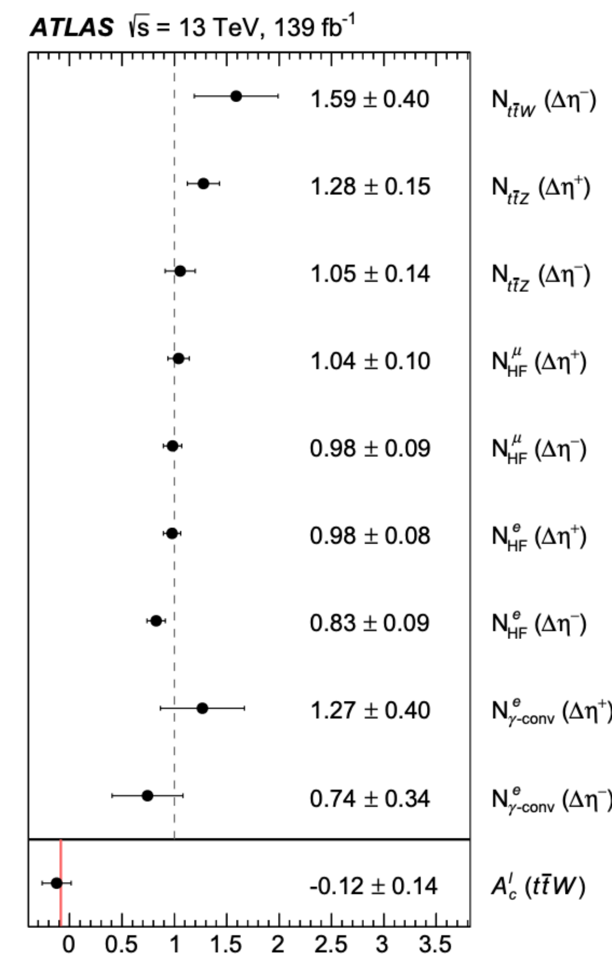

$t\bar{t}W$ charge asymmetry

	Preselection
N_ℓ ($\ell = e/\mu$)	$= 3$
p_T^ℓ ($1^{st}/2^{nd}/3^{rd}$)	≥ 30 GeV, ≥ 20 GeV, ≥ 15 GeV
Sum of lepton charges	± 1
$m_{\ell\ell}^{OSSF}$	≥ 30 GeV

Region-specific requirements				
	SR-1b-lowN_{jets}	**SR-1b-highN_{jets}**	**SR-2b-lowN_{jets}**	**SR-2b-highN_{jets}**
N_{jets}	[2, 3]	≥ 4	[2, 3]	≥ 4
$N_{b\text{-jets}}$	$= 1$	$= 1$	≥ 2	≥ 2
E_T^{miss}	≥ 50 GeV	≥ 50 GeV	–	–
$N_{Z\text{-cand.}}$	$= 0$			
Lepton criteria	TTT			
e/γ ambiguity-cuts	satisfy all			
	CR-$t\bar{t}Z$	**CR-HF$_e$**	**CR-HF$_\mu$**	**CR-γ-conv**
$\ell^{1st/2nd/3rd}$	$\ell\ell\ell$	$\ell\ell e$	$\ell\ell\mu$	$\ell\ell e$, $\ell e\ell$, $e\ell\ell$
N_{jets}	≥ 4	≥ 2	≥ 2	≥ 2
$N_{b\text{-jets}}$	≥ 2	$= 1$	$= 1$	≥ 1
E_T^{miss}	–	< 50 GeV	< 50 GeV	< 50 GeV
$N_{Z\text{-cand.}}$	$= 1$	$= 0$	$= 0$	$= 0$
Lepton criteria	TTT	TT$\bar{\text{T}}$	TT$\bar{\text{T}}$	TTT
e/γ ambiguity-cuts	satisfy all	satisfy all	satisfy all	≥ 1 fail

	$\Delta A_c^\ell(t\bar{t}W)$
Experimental uncertainties	
Jet energy resolution	0.013
Pile-up	0.007
b-tagging	0.005
Leptons	0.004
E_T^{miss}	0.004
Jet energy scale	0.0032
Luminosity	0.0006
MC modelling uncertainties	
$t\bar{t}W$ modelling	0.013
$t\bar{t}Z$ modelling	0.010
HF$_{e/\mu}$ modelling	0.006
$t\bar{t}H$ modelling	0.005
Other uncertainties	
$\Delta\eta^\pm$ CR-dependency	0.05
MC statistical uncertainty	0.019
Data statistical uncertainty	0.14
Total uncertainty	0.15

	$\Delta A_c^\ell(t\bar{t}W)^{PL}$
Experimental uncertainties	
Leptons	0.014
Jet energy resolution	0.011
Pile-up	0.008
Jet energy scale	0.004
E_T^{miss}	0.0015
Luminosity	0.0011
Jet vertex tagger	0.00027
MC modelling uncertainties	
$t\bar{t}W$ modelling	0.022
$t\bar{t}Z$ modelling	0.017
HF$_{e/\mu}$ modelling	0.015
Others modelling	0.015
WZ/ZZ + jets modelling	0.014
$t\bar{t}H$ modelling	0.006
Other uncertainties	
Unfolding bias	0.004
$\Delta\eta^\pm$ CR-dependency	0.04
MC statistical uncertainty	0.027
Response matrix	0.009
Data statistical uncertainty	0.17
Total uncertainty	0.18

$t\bar{t}$ spin correlation

Phys. Rev. D 100 (2019) 072002

$$\tilde{B}_i^{\pm} = b_k^{\pm}\hat{k}_i + b_r^{\pm}\hat{r}_i + b_n^{\pm}\hat{n}_i,$$

$$\begin{aligned}\tilde{C}_{ij} = {} & c_{kk}\hat{k}_i\hat{k}_j + c_{rr}\hat{r}_i\hat{r}_j + c_{nn}\hat{n}_i\hat{n}_j \\ & + c_{rk}(\hat{r}_i\hat{k}_j + \hat{k}_i\hat{r}_j) + c_{nr}(\hat{n}_i\hat{r}_j + \hat{r}_i\hat{n}_j) \\ & + c_{kn}(\hat{k}_i\hat{n}_j + \hat{n}_i\hat{k}_j) + c_n(\hat{r}_i\hat{k}_j - \hat{k}_i\hat{r}_j) \\ & + c_k(\hat{n}_i\hat{r}_j - \hat{r}_i\hat{n}_j) + c_r(\hat{k}_i\hat{n}_j - \hat{n}_i\hat{k}_j).\end{aligned}$$

spin decorrelation D

$$\frac{1}{\sigma}\frac{d\sigma}{d\cos\varphi} = \frac{1}{2}(1 - D\cos\varphi).$$

TABLE I. Observables and their corresponding measured coefficients, production spin density matrix coefficient functions, and P and CP symmetry properties. For the laboratory-frame asymmetries shown in the last two rows, there is no direct correspondence with the coefficient functions.

Observable	Measured coefficient	Coefficient function	Symmetries
$\cos\theta_1^k$	B_1^k	b_k^+	P-odd, CP-even
$\cos\theta_2^k$	B_2^k	b_k^-	P-odd, CP-even
$\cos\theta_1^r$	B_1^r	b_r^+	P-odd, CP-even
$\cos\theta_2^r$	B_2^r	b_r^-	P-odd, CP-even
$\cos\theta_1^n$	B_1^n	b_n^+	P-even, CP-even
$\cos\theta_2^n$	B_2^n	b_n^-	P-even, CP-even
$\cos\theta_1^{k*}$	B_1^{k*}	b_k^+	P-odd, CP-even
$\cos\theta_2^{k*}$	B_2^{k*}	b_k^-	P-odd, CP-even
$\cos\theta_1^{r*}$	B_1^{r*}	b_r^+	P-odd, CP-even
$\cos\theta_2^{r*}$	B_2^{r*}	b_r^-	P-odd, CP-even
$\cos\theta_1^k\cos\theta_2^k$	C_{kk}	c_{kk}	P-even, CP-even
$\cos\theta_1^r\cos\theta_2^r$	C_{rr}	c_{rr}	P-even, CP-even
$\cos\theta_1^n\cos\theta_2^n$	C_{nn}	c_{nn}	P-even, CP-even
$\cos\theta_1^r\cos\theta_2^k + \cos\theta_1^k\cos\theta_2^r$	$C_{rk} + C_{kr}$	c_{rk}	P-even, CP-even
$\cos\theta_1^r\cos\theta_2^k - \cos\theta_1^k\cos\theta_2^r$	$C_{rk} - C_{kr}$	c_n	P-even, CP-odd
$\cos\theta_1^n\cos\theta_2^r + \cos\theta_1^r\cos\theta_2^n$	$C_{nr} + C_{rn}$	c_{nr}	P-odd, CP-even
$\cos\theta_1^n\cos\theta_2^r - \cos\theta_1^r\cos\theta_2^n$	$C_{nr} - C_{rn}$	c_k	P-odd, CP-odd
$\cos\theta_1^n\cos\theta_2^k + \cos\theta_1^k\cos\theta_2^n$	$C_{nk} + C_{kn}$	c_{kn}	P-odd, CP-even
$\cos\theta_1^n\cos\theta_2^k - \cos\theta_1^k\cos\theta_2^n$	$C_{nk} - C_{kn}$	$-c_r$	P-odd, CP-odd
$\cos\varphi$	D	$-(c_{kk} + c_{rr} + c_{nn})/3$	P-even, CP-even
$\cos\varphi_{\mathrm{lab}}$	$A^{\mathrm{lab}}_{\cos\varphi}$	…	…
$\lvert\Delta\phi_{\ell\ell}\rvert$	$A_{\lvert\Delta\phi_{\ell\ell}\rvert}$	…	…

$$\frac{1}{\sigma}\frac{d^2\sigma}{d\cos\theta_1^i\,d\cos\theta_2^j} = \frac{1}{4}(1 + B_1^i\cos\theta_1^i + B_2^j\cos\theta_2^j - C_{ij}\cos\theta_1^i\cos\theta_2^j),$$

$$\frac{1}{\sigma}\frac{d\sigma}{d\cos\theta_1^i} = \frac{1}{2}(1 + B_1^i\cos\theta_1^i),$$

$$\frac{1}{\sigma}\frac{d\sigma}{d\cos\theta_2^i} = \frac{1}{2}(1 + B_2^i\cos\theta_2^i),$$

$$\frac{1}{\sigma}\frac{d\sigma}{dx} = \frac{1}{2}(1 - C_{ij}x)\ln\left(\frac{1}{|x|}\right),$$

$$x = \cos\theta_1^i\cos\theta_2^j.$$

$$\frac{1}{\sigma}\frac{d\sigma}{dx_\pm} = \frac{1}{2}\left(1 - \frac{C_{ij} \pm C_{ji}}{2}x_\pm\right)\cos^{-1}|x_\pm|,$$

$$x_\pm = \cos\theta_1^i\cos\theta_2^j \pm \cos\theta_1^j\cos\theta_2^i.$$

15 observables

$t\bar{t}$ spin correlation

[Phys. Rev. D 100 (2019) 072002]

CMS

TABLE III. Measured coefficients and asymmetries and their total uncertainties. Predicted values from simulation are quoted with a combination of statistical and scale uncertainties, while the NLO calculated values are quoted with their scale uncertainties [3,4]. The NNLO QCD prediction for $A_{|\Delta\phi_{\ell\ell}|}$, with scale uncertainties, is $0.115^{+0.005}_{-0.001}$ [69].

Coefficient	Measured	POWHEGv2	MG5_aMC@NLO	NLO calculation
B_1^k	0.005 ± 0.023	$0.004^{+0.001}_{-0.001}$	$0.000^{+0.001}_{-0.001}$	$4.0^{+1.7}_{-1.2} \times 10^{-3}$
B_2^k	0.007 ± 0.023	$0.006^{+0.001}_{-0.001}$	$-0.002^{+0.001}_{-0.001}$	$4.0^{+1.7}_{-1.2} \times 10^{-3}$
B_1^r	-0.023 ± 0.017	$0.002^{+0.001}_{-0.001}$	$0.002^{+0.001}_{-0.001}$	$1.6^{+1.2}_{-0.9} \times 10^{-3}$
B_2^r	-0.010 ± 0.020	$0.003^{+0.001}_{-0.001}$	$0.000^{+0.001}_{-0.001}$	$1.6^{+1.2}_{-0.9} \times 10^{-3}$
B_1^n	0.006 ± 0.013	$-0.001^{+0.001}_{-0.001}$	$0.001^{+0.001}_{-0.001}$	$5.7^{+0.5}_{-0.4} \times 10^{-3}$
B_2^n	0.017 ± 0.013	$-0.001^{+0.001}_{-0.001}$	$0.000^{+0.001}_{-0.001}$	$5.7^{+0.5}_{-0.4} \times 10^{-3}$
B_1^{k*}	-0.016 ± 0.018	$-0.001^{+0.001}_{-0.001}$	$0.000^{+0.001}_{-0.001}$	$<10^{-3}$
B_2^{k*}	0.007 ± 0.019	$0.001^{+0.001}_{-0.001}$	$0.003^{+0.002}_{-0.001}$	$<10^{-3}$
B_1^{r*}	0.001 ± 0.017	$0.000^{+0.001}_{-0.001}$	$0.000^{+0.001}_{-0.001}$	$<10^{-3}$
B_2^{r*}	0.010 ± 0.017	$0.001^{+0.001}_{-0.001}$	$0.001^{+0.001}_{-0.001}$	$<10^{-3}$
C_{kk}	0.300 ± 0.038	$0.314^{+0.005}_{-0.004}$	$0.325^{+0.011}_{-0.006}$	$0.331^{+0.002}_{-0.002}$
C_{rr}	0.081 ± 0.032	$0.048^{+0.007}_{-0.006}$	$0.052^{+0.007}_{-0.005}$	$0.071^{+0.008}_{-0.006}$
C_{nn}	0.329 ± 0.020	$0.317^{+0.001}_{-0.001}$	$0.324^{+0.002}_{-0.002}$	$0.326^{+0.002}_{-0.002}$
$C_{rk} + C_{kr}$	-0.193 ± 0.064	$-0.201^{+0.004}_{-0.003}$	$-0.198^{+0.004}_{-0.005}$	$-0.206^{+0.002}_{-0.002}$
$C_{rk} - C_{kr}$	0.057 ± 0.046	$-0.001^{+0.002}_{-0.002}$	$0.004^{+0.002}_{-0.002}$	0
$C_{nr} + C_{rn}$	-0.004 ± 0.037	$-0.003^{+0.002}_{-0.002}$	$0.001^{+0.002}_{-0.002}$	$1.06^{+0.01}_{-0.01} \times 10^{-3}$
$C_{nr} - C_{rn}$	-0.001 ± 0.038	$0.002^{+0.002}_{-0.002}$	$0.001^{+0.003}_{-0.002}$	0
$C_{nk} + C_{kn}$	-0.043 ± 0.041	$-0.002^{+0.002}_{-0.002}$	$0.003^{+0.002}_{-0.002}$	$2.15^{+0.04}_{-0.07} \times 10^{-3}$
$C_{nk} - C_{kn}$	0.040 ± 0.029	$-0.001^{+0.002}_{-0.002}$	$-0.001^{+0.002}_{-0.002}$	0
D	-0.237 ± 0.011	$-0.226^{+0.003}_{-0.004}$	$-0.233^{+0.004}_{-0.006}$	$-0.243^{+0.003}_{-0.003}$
$A^{\mathrm{lab}}_{\cos\varphi}$	0.167 ± 0.010	$0.161^{+0.002}_{-0.002}$	$0.174^{+0.004}_{-0.003}$	$0.181^{+0.004}_{-0.003}$
$A_{\vert\Delta\phi_{\ell\ell}\vert}$	0.103 ± 0.008	$0.125^{+0.004}_{-0.005}$	$0.115^{+0.003}_{-0.005}$	$0.108^{+0.009}_{-0.012}$

TABLE V. Summary of the systematic, statistical, and total uncertainties in the extracted $t\bar{t}$ spin correlation coefficients and asymmetries. An ellipsis (···) is shown where the values are <0.0005.

	Uncertainty											
Source	C_{kk}	C_{rr}	C_{nn}	$C_{rk}+C_{kr}$	$C_{rk}-C_{kr}$	$C_{nr}+C_{rn}$	$C_{nr}-C_{rn}$	$C_{nk}+C_{kn}$	$C_{nk}-C_{kn}$	D	$A^{\mathrm{lab}}_{\cos\varphi}$	$A_{\vert\Delta\phi_{\ell\ell}\vert}$
Trigger	0.001	0.001	···	0.002	···	···	···	···	···	···	0.001	···
Lepton ident./iso.	0.001	0.001	···	0.001	···	···	···	···	···	···	···	···
Kinematic reco.	···	···	···	···	···	···	···	···	···	···	···	···
Pileup	0.002	···	0.001	0.004	0.001	0.001	0.002	0.001	0.001	0.001	···	0.001
b tagging	0.004	0.001	0.002	0.005	0.001	0.001	0.001	0.001	0.001	0.001	···	···
JES	0.012	0.009	0.005	0.022	0.011	0.011	0.009	0.012	0.007	0.002	···	0.001
Unclust. energy	0.001	0.001	0.001	0.004	0.001	0.001	0.002	0.001	0.001	···	···	0.001
JER	0.001	0.002	0.001	0.004	0.002	0.001	0.001	0.003	0.001	···	···	···
Scales	0.012	0.006	0.007	0.026	0.011	0.007	0.014	0.011	0.007	0.003	0.002	0.003
ME/PS matching	0.004	0.003	0.001	0.009	0.016	0.011	0.001	0.012	0.009	0.002	0.002	0.004
Color reconnect.	0.005	0.013	0.006	0.013	0.011	0.014	0.017	0.009	0.008	0.002	0.001	0.001
Underlying event	0.008	0.002	0.002	0.004	0.010	0.007	0.005	0.007	0.002	0.003	0.001	0.001
b quark fragment.	0.014	0.002	0.005	0.017	0.001	0.001	0.001	0.002	0.001	0.003	···	0.001
b had. semilep. d.	···	0.001	0.001	0.002	···	0.001	···	···	···	0.001	···	···
PDF	0.002	0.002	0.001	0.002	···	···	···	···	···	0.001	0.003	0.001
Top quark mass	0.001	0.002	0.006	0.006	0.009	0.002	0.002	0.009	0.001	0.002	0.001	···
Top quark p_{T}	0.008	0.011	0.005	0.019	···	0.001	···	0.001	···	0.004	0.003	0.005
Background	0.017	0.009	0.008	0.025	0.006	0.004	0.004	0.007	0.003	0.004	0.008	0.002
Total systematic	0.031	0.023	0.016	0.053	0.029	0.024	0.025	0.026	0.016	0.009	0.010	0.007
Data statistical	0.018	0.019	0.010	0.029	0.029	0.024	0.025	0.025	0.020	0.006	0.003	0.003
Signal sim. stat.	0.007	0.007	0.004	0.011	0.011	0.009	0.009	0.010	0.008	0.002	0.001	0.001
Bkg. sim. stat.	0.010	0.010	0.005	0.018	0.017	0.012	0.010	0.015	0.012	0.003	0.002	0.002
Total statistical	0.022	0.023	0.012	0.035	0.035	0.028	0.028	0.031	0.025	0.007	0.003	0.003
Total	0.038	0.032	0.020	0.064	0.046	0.037	0.038	0.041	0.029	0.011	0.010	0.008

Top polarisation

Uncertainty source	$\Delta P^{t}_{x'}$	$\Delta P^{\bar{t}}_{x'}$	$\Delta P^{t}_{y'}$	$\Delta P^{\bar{t}}_{y'}$	$\Delta P^{t}_{z'}$	$\Delta P^{\bar{t}}_{z'}$
Modelling						
Modelling (t-channel)	±0.037	±0.051	±0.010	±0.015	±0.061	±0.061
Modelling ($t\bar{t}$)	±0.016	±0.021	±0.004	±0.016	±0.003	±0.016
Modelling (other)	±0.013	±0.031	±0.003	±0.006	±0.026	±0.043
Experimental						
Jet energy scale	±0.045	±0.048	±0.005	±0.007	±0.033	±0.025
Jet energy resolution	±0.166	±0.185	±0.021	±0.040	±0.070	±0.130
Jet flavour tagging	±0.004	±0.002	<0.001	±0.001	±0.007	±0.009
Other experimental uncertainties	±0.015	±0.029	±0.002	±0.007	±0.014	±0.026
Multijet estimation	±0.008	±0.021	<0.001	±0.001	±0.008	±0.013
Luminosity	±0.001	±0.001	<0.001	<0.001	<0.001	<0.001
Simulation statistics	±0.020	±0.024	±0.008	±0.015	±0.017	±0.031
Total systematic uncertainty	±0.174	±0.199	±0.025	±0.048	±0.096	±0.153
Total statistical uncertainty	±0.017	±0.025	±0.011	±0.017	±0.022	±0.034

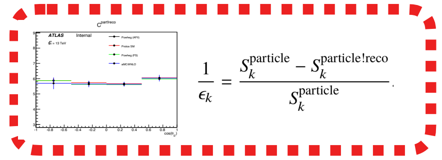

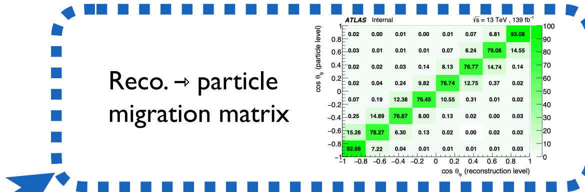

$$N_k^{particle} = C_k^{particle!reco} \sum_j M^{-1}_{jk} C_j^{reco!particle} (N_j^{data} - B_j)$$

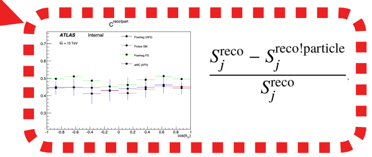

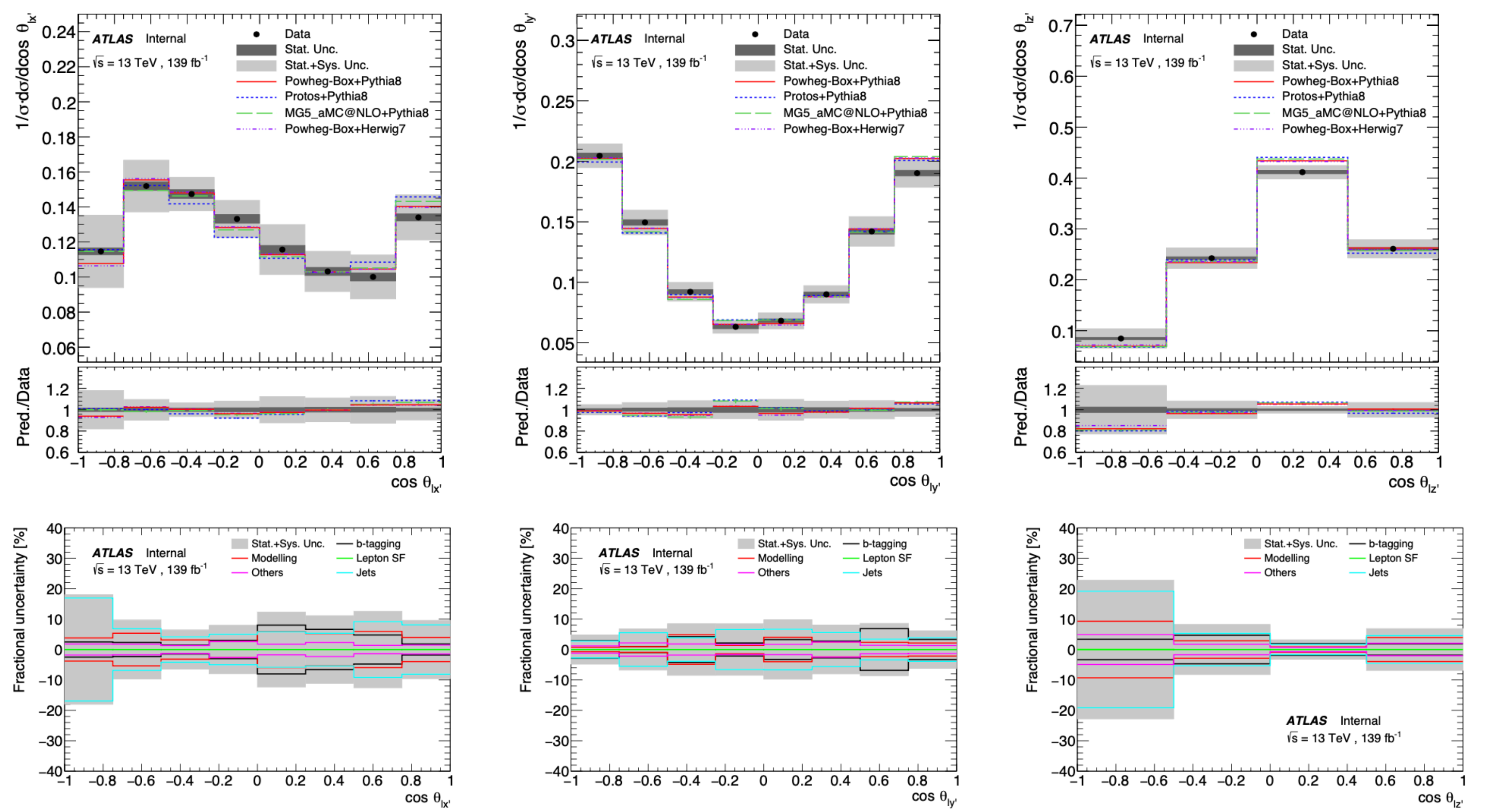

Top polarisation

$$\sigma\left(\frac{c}{\Lambda^2}\right) = \underbrace{O_{\mathrm{SM}}^2}_{\text{Pure SM}} + \frac{c}{\Lambda^2}\cdot \underbrace{O_{\mathrm{SM}}O_{\mathrm{dim6}}}_{\text{Interference term}} + \frac{c^2}{\Lambda^4}\cdot \underbrace{O_{\mathrm{dim6}}^2}_{\text{Pure BSM}}$$

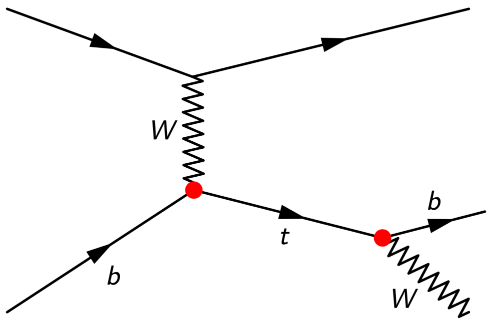

EFT operator can contribute to production and/or decay vertex

3 operators that interfere with SM: $\boldsymbol{O_{\phi Q}}$, $\boldsymbol{O_{tW}}$ *and* $\boldsymbol{O_{qQ}}$

- four couplings: $\boldsymbol{C_{\phi Q}}$, $\boldsymbol{C_{tW}}$, $\boldsymbol{C_{itW}}$ and $\boldsymbol{O_{qQ}}$
- $C_{tW}^* \neq C_{tW}$ → CP Violation
- prediction @NLO available: arXiv:1807.03576

Interpretation of normalized cosθ$_{X/Y}$ focuses on C_{tW} and C_{itW}

- $O_{\phi Q}$ affects only normalisation
- cosθ$_{X/Y}$ not sensitive to O_{qQ}

Morphing reference: ATL-PHYS-PUB-2015-047

- Morphing works with any choice of templates
- Uncertainty does depend on this choice

	C_{tW} 68% CL	C_{tW} 95% CL	C_{itW} 68% CL	C_{itW} 95% CL
All terms	[-0.2, 0.9]	[-0.7, 1.5]	[-0.5, -0.1]	[-0.7, 0.2]
Order $1/\Lambda^4$	[-0.2, 0.9]	[-0.7, 1.5]	[-0.5, -0.1]	[-0.7, 0.2]
Order $1/\Lambda^2$	[-0.2, 1.0]	[-0.7, 1.7]	[-0.5, -0.1]	[-0.8, 0.2]

IBU vs. FBU vs. SVD vs. PLU

Reference: arxiv.org/1201.4612

FBU differs from *D'Agostini's iterative unfolding (IBU)* despite both using Bayes' theorem.

- In FBU the answer is not an estimator and its covariance matrix, but a posterior probability density defined in the space of possible spectra.
- FBU does not involve iterations, thus does not depend on a convergence criterion, nor on the first point of an iterative procedure, which in IBU is named "prior".
  + If more than one answers are equally likely, as can happen when the reconstructed spectrum has fewer bins than the inferred one, then FBU reveals all of them, while IBU converges towards some of the possible solutions.
- Regularization is not done by interrupting iterations, but by choosing a prior which favours certain characteristics, such as smoothness.
  + Thus, FBU offers intuition and full control of the regularizing condition, which makes the answer easy to interpret.

FBU differs significantly also from *SVD unfolding*.

- In FBU the migrations matrix is not distorted by singular value decomposition (SVD), therefore FBU assumes the intended migrations model.
- The answer of FBU is not an estimator plus covariance matrix, but a probability density function which does not have to be Gaussian, which is important especially in bins with small Poisson event counts.
- FBU does not involve matrix inversion and computation of eigenvalues, which makes it more stable numerically.
- SVD imposes curvature regularization, while FBU offers the freedom to use different regularization choices. This freedom becomes necessary when the correct answer actually has large curvature, or when the answer has only two bins, thus curvature is not even defined.

PLU is similar to *FBU* in terms of prior for regularisation, but it involves a Profile Likelihood fit too.